Journal of the

ENGINEERING MECHANICS DIVISION

Proceedings of the American Society of Civil Engineers

CONTENTS

April, 1959

Papers

Journal of the
ENGINEERING MECHANICS DIVISION
Proceedings of the American Society of Civil Engineers

COLUMNS UNDER COMBINED BENDING AND THRUST

Theodore V. Galambos,[1] J.M. ASCE and Robert L. Ketter,[2] J.M. ASCE

SYNOPSIS

Interaction curves relating the axial thrust, applied end bending moment and slenderness ratio are developed for the ultimate carrying capacity of pin-ended, wide-flange beam-columns. It is assumed that failure is due to excessive bending in the plane of the applied moments which is further considered to be the plane of the web. The two conditions of loading that are investigated are (1) equal end moments applied such that the resulting deformation is one of single curvature, and (2) end moment applied only at one extremity of the member. The influence of an assumed symmetrical residual stress pattern is considered in the calculations and curves are presented for slenderness ratios up to and including $L/r = 120$. For ease of future computations, the interaction curves are fitted into approximate equations. Comparisons are made with various column test results.

I. INTRODUCTION

When designing (or analyzing) a structure by the simple plastic theory, it is assumed that the member in question will deliver the fully plastic moment value, M_p, noted in the calculations. This, however, will not necessarily be the case if the member is subjected to an axial thrust in addition to bending moments.(1) To attain the desired moment value, it is necessary to supply a member having a greater fully plastic moment value than the one needed for pure bending; i.e., one that will develop the required end moment in the presence of the imposed axial thrust. The results of this report then apply without modification to rolled wide-flange columns of A-7 structural steel. Similar procedures could be used for other materials and loading conditions.

Note: Discussion open until September 1, 1959. To extend the closing date one month, a written request must be filed with the Executive Secretary, ASCE. Paper 1990 is part of the copyrighted Journal of the Engineering Mechanics Division, Proceedings of the American Society of Civil Engineers, Vol. 85, No. EM 2, April, 1959.

1. Research Associate, Fritz Eng. Lab., Lehigh Univ., Bethlehem, Pa.
2. Prof. and Head, Dept. of Civ. Eng. Univ. of Buffalo, Buffalo, N. Y.; formerly of Fritz Eng. Lab., Lehigh Univ., Bethlehem, Pa.

However, to afford a means of comparing test results with predicted strengths and to facilitate solution of problems where the material has a yield point other than 33,000 psi, a method of modifying the solution is presented in Section IV.

The problem that will be considered in this paper is the determination of the maximum amount of end bending moment that a member can sustain when it is also subjected to a given axial thrust; the material presented herein constitutes an extension of certain of the ideas advanced in an earlier paper.(2) Two loading cases will be investigated:

1. axial thrust plus equal end moments applied at both ends of the member such that it deforms in single curvature, and
2. axial thrust plus moment applied only at one end of the member.

These conditions are shown diagrammatically as loading conditions "c" and "d" in Fig. 1. In both cases it is assumed that the plane of the applied

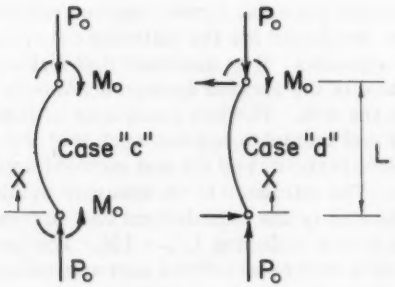

Fig. 1 CONDITIONS OF LOADING

moments is that of the web of the section and that failure is the result of excessive bending in this same plane.

The stress-strain properties of the material are pre-supposed to be ideally elastic-plastic; i.e., there is initially a linear range wherein $\sigma = E\epsilon$ which is followed by a constant stress level $\sigma = \sigma_y$ for strains greater than ϵ_y.* This type of behavior is typical of mild structural (ASTM A7) steel if strain-hardening is neglected. There is, however, assumed to be a symmetrical residual stress pattern present in the member prior to the application of any external loads. The presumed pattern (Fig. 2) is consistent with measured residual stresses in wide-flange column type sections resulting from cooling of the section during and after rolling.(2), (3)

As shown in Ref. 2, if the material is homogeneous and isotropic and if bending strains are assumed to be proportional to the distance from the neutral axis, then the thrust-moment-curvature relationship for the 8WF31 section will be that given in Fig. 3. In this figure two conditions are illustrated. The solid lines are for the cases where residual stresses are neglected.

* The nomenclature is given in Section VIII.

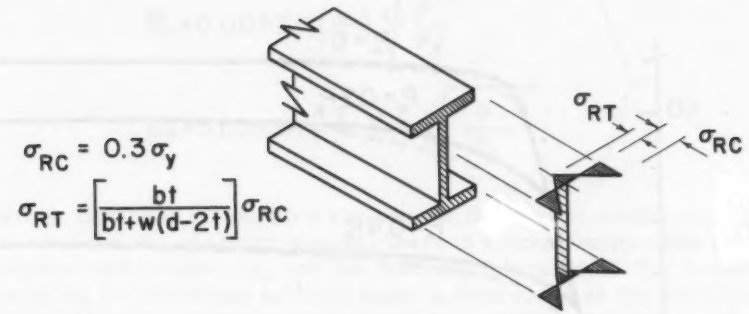

Fig.2 ASSUMED COOLING RESIDUAL STRESS PATTERN

The solutions which include the influence of the residual stress pattern shown in Fig. 2 are given by the dashed lines in Fig. 3.

Since the basic approach that will be used in solving the problem considered in this paper is one of numerical integration, and since this integration will proceed from a knowledge of the curvature values of Fig. 3, which, as was stated above, were computed for the 8WF31 section, the resulting interaction curves will in the strictest sense apply only to the 8WF31 section. It should be noted, however, that this section has one of the more severe thrust-moment-curvature relationships of the column sections rolled because of its low shapefactor (1.11 as compared to 1.14 for most sections.) Using the interaction curves for other shapes should therefore result in a somewhat conservative or at least equal prediction of strength for the member in question.

For ease of presentation and generalization, load and section property parameters have been non-dimensionalized wherever possible. It was necessary, however, to consider a fixed value of Young's Modulus of E = 30,000,000 psi. Since specifications require a minimum yield stress of σ_y = 33,000 psi for A7 steels, this value was used in the calculations as the base yield stress. (A)

II. Determination of Interaction Curves

The approach that will be used in the solution of the problem in question will be one of numerical integration.[4] The calculation will proceed from an assumed deflection configuration and will take into account the non-linearity between moment and curvature as strains exceed the initial yield strain.

Since deflections must be assumed, it is desirable to know the equation of the column centerline at initiation of yielding for each of the conditions of loading. These can be determined from a consideration of the equations on page 12 of Ref. 5. In terms of the parameters used in this report, the equations are as follows:

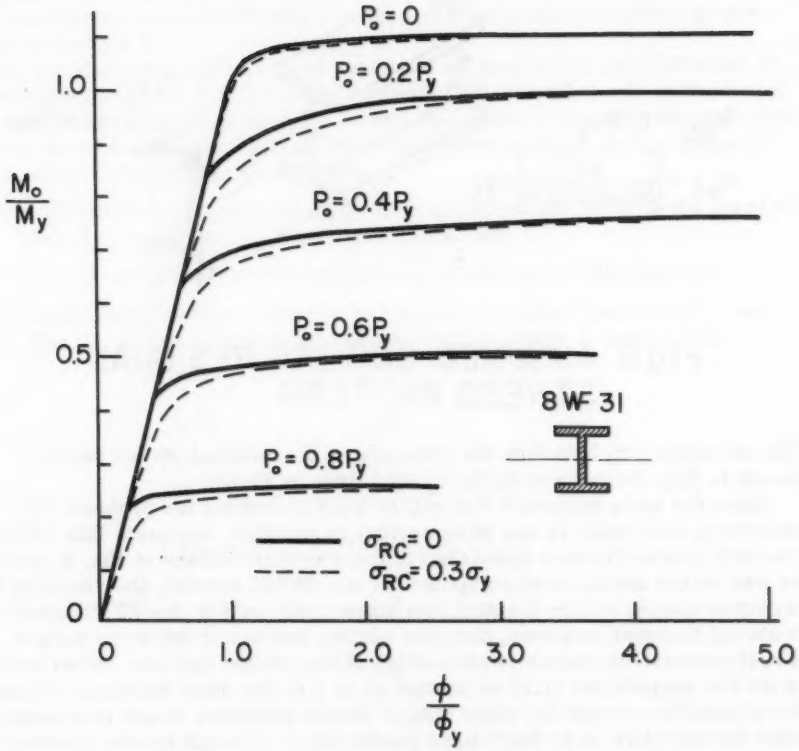

Fig. 3 MOMENT-THRUST-CURVATURE RELATIONSHIP, INCLUDING INFLUENCE OF RESIDUAL STRESS[2]

a) Moments applied at both ends of the member, (condition "c" in Ref. 2)

$$(L/r)_{adj.} = L/r\sqrt{\frac{\sigma_y}{33{,}000}} \qquad (1)$$

b) Moment applied only at one end of the member (condition "d" in Ref. 2)

$$y = \frac{S}{A}\left[\frac{M_o/M_p}{P/P_y}\right]\left[\frac{\sin kx}{\sin kL} + \cos kx - \cot kL \sin kx - 1\right] \qquad (2)$$

For the assumed values of E = 30,000,000 psi and σ_y = 33,000 psi

$$\left.\begin{aligned} kL &= 0.003317\left(\frac{L}{r}\right)\sqrt{\frac{P}{P_y}} \\ kx &= 0.003317\left(\frac{x}{L}\right)\left(\frac{L}{r}\right)\sqrt{\frac{P}{P_y}} \end{aligned}\right\} \qquad (3)$$

From Equations (1) and (2) it can be seen that for the conditions of constant axial thrust and elastic behavior there is a linear relationship between the applied end moment, M_o, and the resulting deformation. The maximum value of M_o for which this situation holds is referred to as the initial yield value and the solution to this problem has been presented in Ref. 6 and elsewhere. For greater values of applied end moment yielding will occur at the most highly strained sections along the member. In these regions the member becomes relatively weaker to further increases in loading. This can be seen from the moment-curvature diagrams of Fig. 3. The load-deformation relationship of the member as a whole will also indicate this decrease in stiffness but in the early stages at a less pronounced rate. This follows from the fact that the total deformation is the integrated effect of all of the curvature values along the length of the member.

To be able to determine the maximum carrying capacity of a given member, it is essential that the load-deformation relationship of that particular member be defined. But since, as was noted earlier, a numerical integration procedure is to be used,[4] it is first necessary to assume deflection values along the member and successively correct these assumptions based on the corresponding integrated curvature values. The process must be repeated until the desired accuracy of the deflected shape is obtained. For any one member and axial thrust ratio, then, the definition of the load-deformation relationship above the elastic limit, and thereby the definition of the critical loading, may require the consideration of four or five end moment values which in turn may require three or four numerical integrations each.

In addition, for a given slenderness ratio, it is necessary to determine the critical value of the end moment for various values of the axial thrust. This would make it possible to define the relationship between axial thrust and end moment for this one particular slenderness value; i.e., to define the interaction curve for this given slenderness ratio. In general $0.2\ P_o/P_y$ intervals were used in the computations on which the interaction curves of this report are based. For a better definition of the relationship at higher values of thrust, however, a closer spacing of values of P_o/P_y had to be used. Slenderness ratios ranging from 0 to 120 were considered in intervals of 20.

In outline form, then, the steps that were used in determining each of the interaction curves presented in this report are as follows:

GIVEN: loading condition, slenderness ratio and constant axial thrust value, for the 8WF31 Section used as a standard.

1. Assume an end moment, M_o, greater than the initial yield value;
2. Assume a possible deflection configuration; (as a first approximation, the elastic limit deflections defined by Equations (2) and (3) could be used; however, this is not necessary. Any reasonable assumption of deflection would be satisfactory.)

3. Computing the moment values at eight equally spaced stations along the length of the member ($M_x = M_o + P_{oy}$) and numerically integrate curvature values obtained from Fig. 3 (an enlarged version of this figure was used). Figure 5 shows a complete cycle of numerical integration.
4. Correct the assumed deflections based on the values obtained from this numerical integration and repeat step (3);
5. Repeat step (4) until the desired accuracy is obtained ($\pm$ 0.001 inch was used in this report);

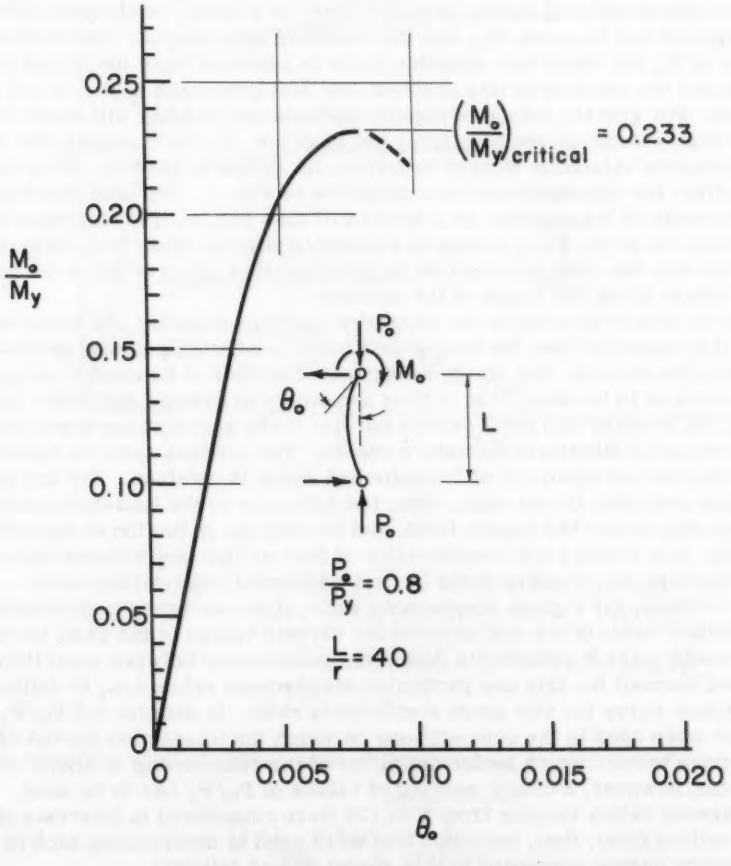

Fig. 4 TYPICAL MOMENT VERSUS END ROTATION CURVE

Given: $\frac{L}{r_x} = 40$; $\frac{P_o}{P_y} = 0.8$; 8WF31 Section; L = 138.8"; λ = 17.35"

Assumed: $\frac{M_o}{M_y} = 0.2$

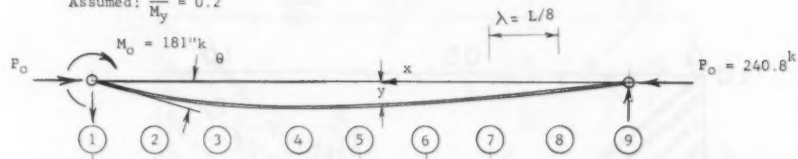

First Trial

										MF*	Notation
a	181	158	136	113	90	68	45	23	0		Moment due to M_o
b	0	0.026	0.049	0.068	0.047	0.044	0.032	0.008	0		Assumed Deflection
c	0	5	10	14	10	9	7	2	0		Moment due to P_o
d	181	163	146	127	100	77	52	25	0		Total Moment (a + c)
e	0.200	0.180	0.161	0.140	0.111	0.085	0.058	0.028	0		M_x/M_y
f	0.350	0.290	0.250	0.210	0.151	0.119	0.083	0.045	0	$\lambda\phi_y$	Concentrated Angle Changes **
g		0.350	0.640	0.890	1.100	1.251	1.370	1.453	1.498	$\lambda\phi_y$	Slope
h	0	0.350	0.990	1.880	2.980	4.231	5.601	7.045	8.552	$\lambda^2\phi_y$	Deflection
i	0	1.069	2.138	3.207	4.276	5.345	6.141	7.483	8.552	$\lambda^2\phi_y$	Correction to Deflection
j	0	0.719	1.143	1.327	1.296	1.114	0.540	0.429	0	$\lambda^2\phi_y$	Final Deflection
k	0	0.060	0.095	0.110	0.107	0.092	0.045	0.036	0		Final Deflection in Inches

Fourth Trial

										Notation
a'	0	0.069	0.112	0.131	0.129	0.112	0.081	0.043	0	Assumed Deflection***
k'	0	0.070	0.113	0.132	0.130	0.112	0.082	0.043	0	Final Deflection

* Multiplication Factor
** From Fig. 3, corresponding to $\frac{M_x}{M_y}$

*** Line k from third trial = line a' of fourth trial

The corresponding endslope $\theta = \frac{4x0.070-0.113}{2x17.35} = 0.00481$

Fig. 5 TYPICAL NUMERICAL INTEGRATION PROCEDURE TO OBTAIN END SLOPE

6. Determine the end rotation for the final deflection values of step (5)*

* If it is assumed that the deflection curve of the member within the three end segments can be represented by a parabola, then the end slope can be expressed in terms of the known deflection as

$$\theta = \frac{4\delta_1 - \delta_2}{2\lambda} \qquad (4)$$

where

δ_1 = deflection at first station away from the applied moment end of

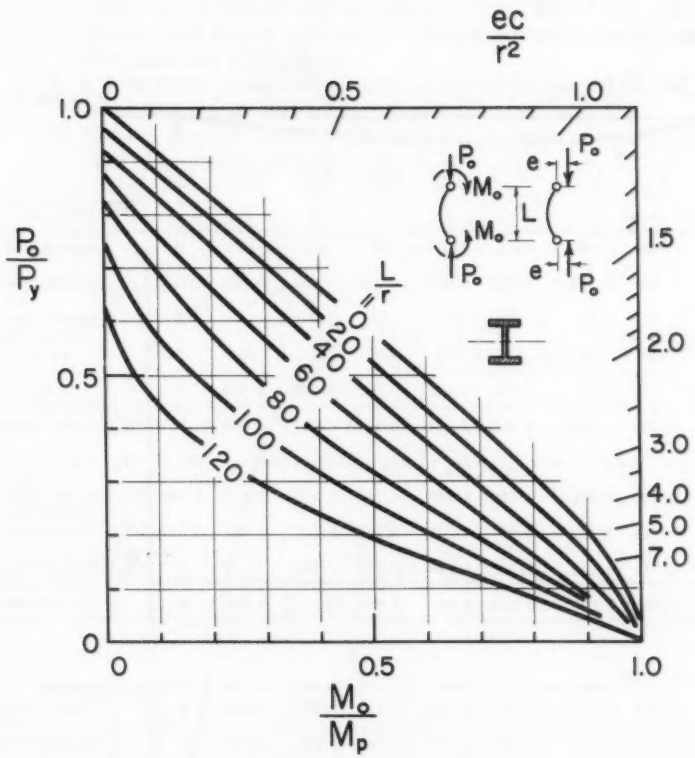

Fig. 6 MAXIMUM CARRYING CAPACITY INTERACTION CURVES (INCLUDING THE INFLUENCE OF RESIDUAL STRESS) CONDITION "c" LOADING

7. Assume greater values of the end moment, M_0, and repeat the same process as outlined above;**
8. Plot the various values of M_0 versus θ_0 from step (7) and determine the maximum value of M_0 from the resulting curve. (See Fig. 4).

---

the member,

δ_2 = deflection at the second station away from the applied moment end of the member, and

λ = grid spacing (assumed to be L/8 for the cases considered).

** If an M_0 greater than or equal to M_0(critical)is assumed, the numerical integration process yields divergent results.

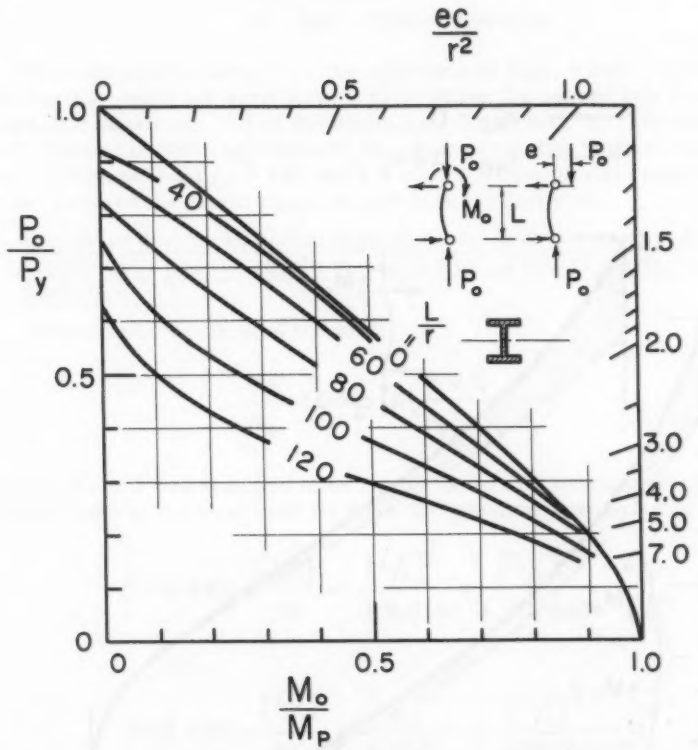

Fig. 7 MAXIMUM CARRYING CAPACITY INTERACTION CURVES (INCLUDING THE INFLUENCE OF RESIDUAL STRESS) CONDITION "d" LOADING

This gives one particular point on one particular interaction curve. As was pointed out above, it is necessary to determine many such points to be able to define the desired range of the interaction curves.

Dividing the $(M_o/M_y)_{critical}$ values obtained from the numerically determined M_o versus θ_o curves by the shape-factor (i.e., $\frac{M_p}{M_y}$), the interaction curves of P_o/P_y versus M_o/M_p versus L/r shown in Figs. 6 and 7 were obtained. Fig. 6 is for the case of moments applied at both ends of the member (condition "c") and Fig. 7 is for the case of moment applied at one end (condition "d"). Only the interaction curves incorporating the influence of residual stress have been included in this report. However, interaction curves neglecting these stresses as well as the corresponding initial yield interaction curves are shown in Ref. 7. Also given therein is a more detailed explanation of the derivation of the curves shown in Figs. 6 and 7. To give an indication of the influence of residual stress on the carrying capacity of

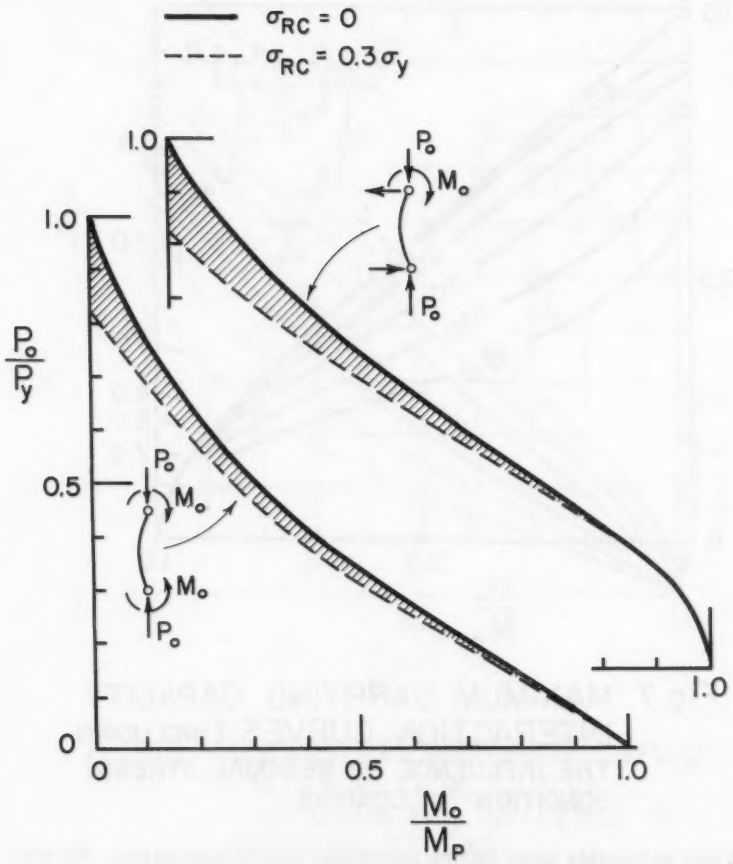

Fig. 8 INTERACTION CURVES FOR $\frac{L}{r}=80$ SHOWING INFLUENCE OF RESIDUAL STRESS

members of the type considered herein, Fig. 8 gives comparable interaction curves for an $L/_r = 80$.

To make the curves more useful when eccentricity ratios (ec/r^2) are given instead of end moments, values of ec/r^2 are also shown on the interaction curve figures.

III. Approximate Equations

To avoid interpolating from the diagrams of Figs. 6 and 7, approximate interaction equations were developed by fitting the curves into cubic and quadratic equations. All of the limitations of the original curves are therefore present in these approximations. In general, the range of application was chosen as $0 \leq L/r \leq 120$ and $0 \leq P_o/P_y \leq 0.6$. It was considered that these covered the major range of practical applications.

1. Pin-ended column subjected to axial thrust plus two equal end-moments applied such that the resulting deformation is that of single curvature (condition "c"):

   Assuming an equation of the form

$$\frac{M_o}{M_p} = 1.000 - K\left(\frac{P}{P_y}\right) - J\left(\frac{P}{P_y}\right)^2 \tag{5}$$

where K and J are assumed to be functions only of the slenderness ratio, the coefficients of the axial load terms of the equation were found to be

$$\left.\begin{aligned} K &= 0.420 + \frac{(L/r)}{70} - \frac{(L/r)^2}{29{,}000} + \frac{(L/r)^3}{1{,}160{,}000} \\ J &= 0.770 - \frac{(L/r)}{60} + \frac{(L/r)^2}{8{,}700} - \frac{(L/r)^3}{606{,}000} \end{aligned}\right\} \tag{6}$$

The agreement between these expressions and the comparable relationship from Fig. 6 is as shown in Fig. 9. The solid lines of Fig. 9 are obtained by matching Equ. (5) to two points of each curve on Fig. 6. The direct correlation between values obtained from the approximate equations (shown as points) and the interaction curves of Fig. 6 is given in Fig. 10.

1. Pin-ended column subjected to axial thrust plus an end-moment applied only at one end of the member (condition "d"):

   Assuming an equation of the form

$$\frac{M_o}{M_p} = B - G\left(\frac{P}{P_y}\right) \tag{7}$$

where (as in case 1) B and G are assumed to be functions only of the slenderness ratio, the coefficients are found to be

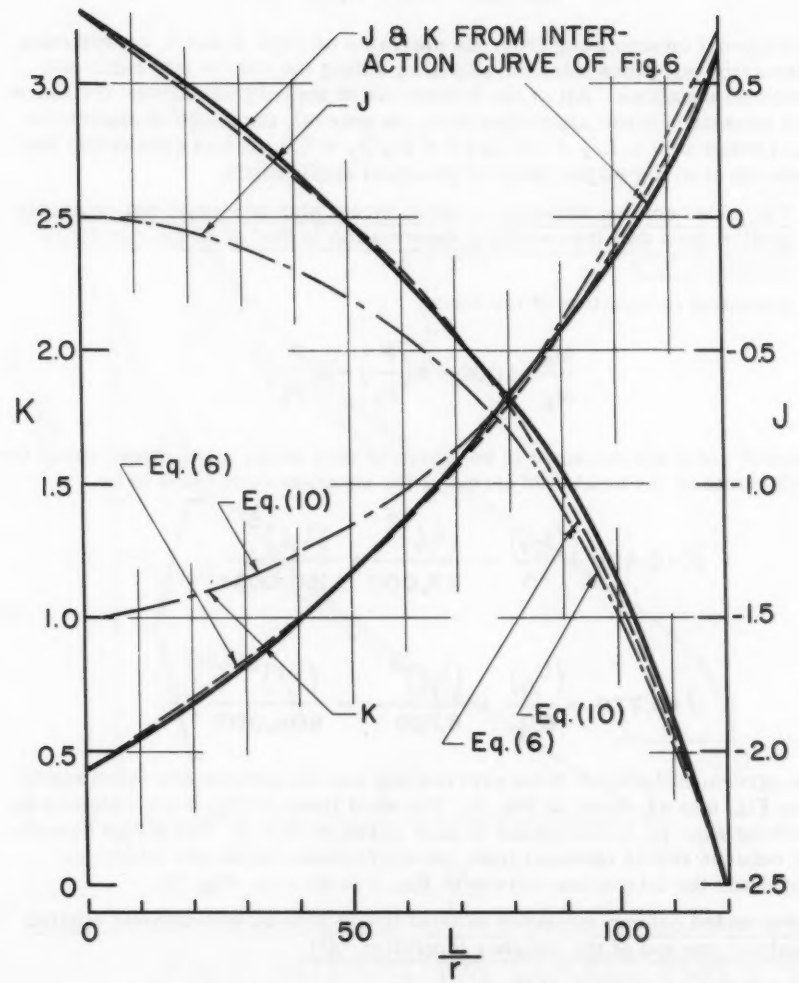

Fig.9 COEFFICIENTS FOR LOADING CONDITION "c" INTERACTION CURVES

$$\left.\begin{aligned} G &= 1.110 + \frac{(L/r)}{190} - \frac{(L/r)^2}{9{,}000} + \frac{(L/r)^3}{720{,}000} \\ B &= 1.133 + \frac{(L/r)}{3080} + \frac{(L/r)^2}{185{,}000} \end{aligned}\right\} \quad (8)$$

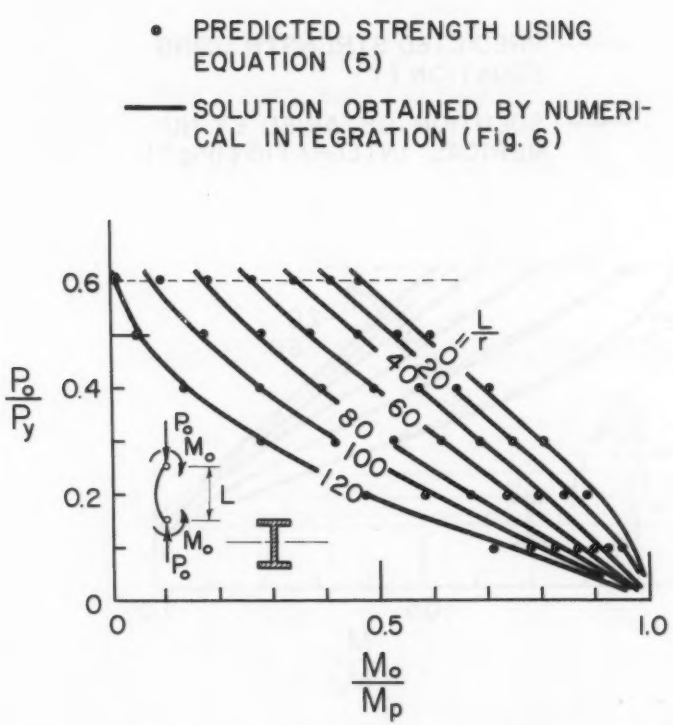

Fig. 10 COMPARISON BETWEEN "EXACT" AND "APPROXIMATE" INTERACTION CURVES (LOADING CONDITION "c")

It should be noted that when Equation (7) predicts a value of M_o/M_p greater than 1.00 (that is, for small values of P_o/P_y), $M_o/M_p = 1.00$ should be used.

The agreement between the approximate interaction Equation (7) and the relationships determined numerically (Fig. 7) is shown in Fig. 11.

Table 1 is a tabulation of the interaction equation constants B, G, J and K for L/r values from 0 to 120 varying in increments of 5.

3. "C.R.C. Interaction Equation"

Recently, attention has been focused on the application of the so-called "C.R.C. interaction equation" to the first ("c") condition of loading.(8)(11)

$$\frac{P}{P'} - \frac{M_o/M'}{1 - P/P_e} = 1 \qquad (9)$$

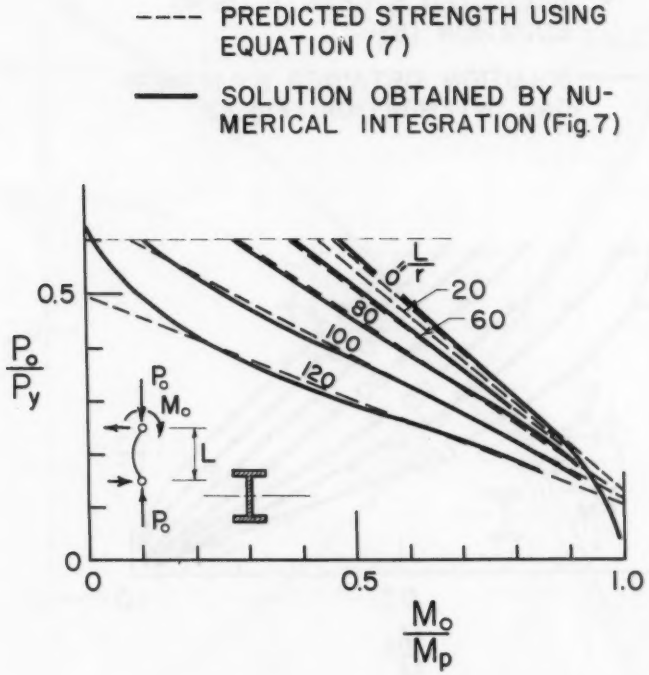

Fig.11 COMPARISON BETWEEN "EXACT" AND "APPROXIMATE" INTERACTION CURVES (LOADING CONDITION "d"

where

P' = maximum axial thrust that the member will sustain when subjected to pure axial thrust;
M' = maximum end moment that the member will sustain when subjected to pure bending; and
P_e = Euler buckling load for the axially loaded member.

Since it was assumed in the derivation of the interaction curves presented earlier in this report that the member did not fail by lateral instability, M' of Equation (9) should be taken equal to M_p. Equation (9) then becomes

$$\frac{M_o}{M_p} = 1.000 - K'\left(\frac{P}{P_y}\right) - J'\left(\frac{P}{P_y}\right)^2$$

TABLE 1

CONSTANTS FOR INTERACTION CURVE EQUATIONS

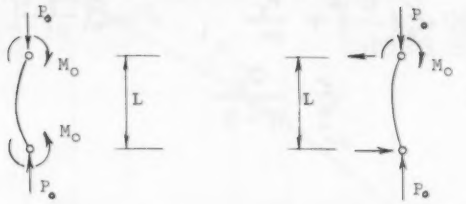

Loading Condition "c" | Loading Condition "d" *

$$\frac{M_o}{M_p} = 1.0 - K\left(\frac{P_o}{P_y}\right) - J\left(\frac{P_o}{P_y}\right)^2 \qquad \frac{M_o}{M_p} = B - G\left(\frac{P_o}{P_y}\right)$$

$\frac{L}{r}$	Condition "c"		Condition "d" *	
	K	J	G	B
0	0.42	0.77	1.11	1.13
5	0.49	0.69	1.13	1.14
10	0.56	0.61	1.15	1.14
15	0.63	0.53	1.17	1.14
20	0.70	0.46	1.18	1.14
25	0.77	0.39	1.19	1.14
30	0.85	0.31	1.21	1.15
35	0.92	0.24	1.22	1.15
40	0.99	0.17	1.23	1.16
45	1.08	0.08	1.25	1.16
50	1.17	-0.01	1.27	1.16
55	1.26	-0.10	1.29	1.17
60	1.35	-0.21	1.32	1.17
65	1.45	-0.32	1.36	1.18
70	1.56	-0.44	1.41	1.18
75	1.68	-0.57	1.46	1.19
80	1.81	-0.72	1.52	1.19
85	1.93	-0.88	1.60	1.20
90	2.07	-1.05	1.69	1.21
95	2.22	-1.24	1.79	1.21
100	2.38	-1.45	1.90	1.22
105	2.55	-1.68	2.03	1.23
110	2.74	-1.93	2.18	1.23
115	2.94	-2.20	2.34	1.24
120	3.16	-2.51	2.53	1.25

*Note: For calculated values of $\frac{M_o}{M_p} > 1.0$, use $\frac{M_o}{M_p} = 1.00$

where

$$K' = \xi\left(\frac{L}{r}\right)^2 + \frac{P_y}{P'} \quad ; \quad J' = -\xi\left(\frac{P_y}{P'}\right)\left(\frac{L}{r}\right)^2 \qquad (10)$$

and

$$\xi = \frac{\sigma_y}{\pi^2 E}$$

In Fig. 9, the expressions for K' and J' (determined from Equations 10 using for (P'/P_y) the end points for the case where $\frac{M_o}{M_p} = 0$ of Fig. 6 or 7) are compared with the values determined by numerical integration.

4. Axially Loaded Columns

Approximating that portion of the relationship between axial thrust and slenderness ratio that occurs below the Euler curve (that is, $0 \leq L/r \leq 112$), the following expression may be used

$$\frac{P}{P_y} = 1.000 - \frac{(L/r)}{645} - \frac{(L/r)^2}{111{,}000} \qquad (11)$$

Since this equation almost coincides with the numerically determined values shown in Figs. 6 and 7 where $M_o/M_p = 0$, a comparison has not been shown.

It is gratifying to note the close correspondence between Equation (11) of this paper and Equation (20) of Ref. 17 by Bijlaard, Fisher and Winter, since the latter expression was determined by an entirely different procedure.

IV. Comparison with Test Results

As an experimental check of the theoretical predictions of this report, existing test data are compared with the interaction curves of Figs. 6 and 7. The tests of the following experimental programs are used for comparison:

1. Cornell University, 1956 (Ref. 9)
2. Lehigh University, 1940 (Ref. 10)
3. University of Liege, 1956 (Refs. 11, 12)
4. University of Wisconsin, 1920's (Ref. 13)
5. Lehigh University, current series (Refs. 2, 6)

Graphs comparing the analytical predictions with experimental results are shown in Figs. 12, 13, 14, 15 and 16.

---

* For A-7 Steel, $= \frac{33{,}000}{\pi^2 (30 \times 10^6)} = 1.113 \times 10^{-5}$

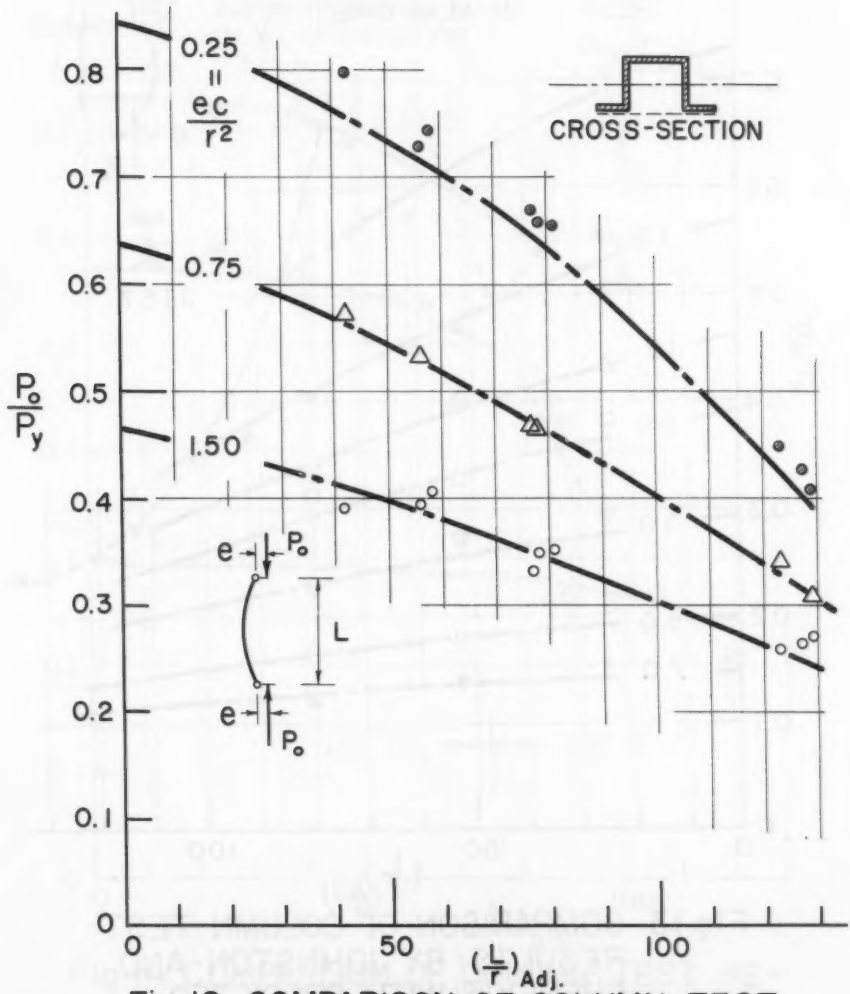

Fig. 12 COMPARISON OF COLUMN TEST RESULTS BY MASON, FISHER AND WINTER[9] WITH PREDICTED STRENGTHS

When comparing the theoretical results with the experiments, it was necessary to adjust the slenderness ratio. This was done in the following manner:

$$\text{Euler Equation} - \left(\frac{L}{r}\right)^2 = \frac{\pi^2 E}{\sigma_y \left(\frac{P_o}{P_y}\right)} \quad , \qquad (11)$$

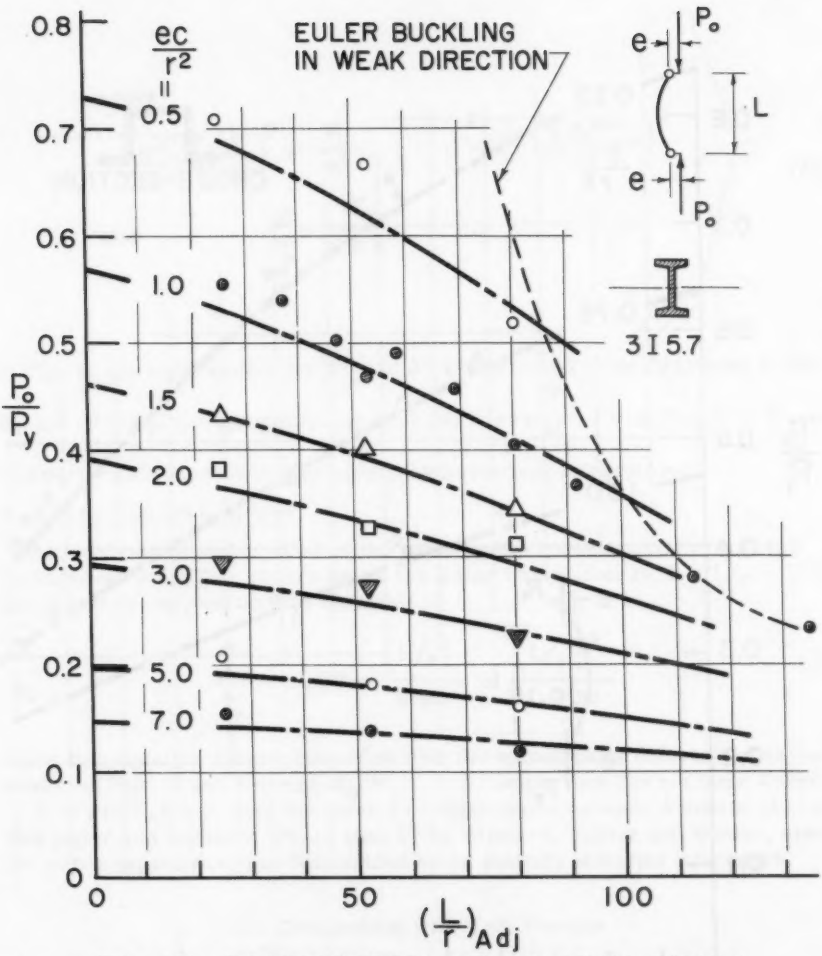

Fig. 13 COMPARISON OF COLUMN TEST RESULTS BY JOHNSTON AND CHENEY[10] WITH PREDICTED STRENGTHS

$$\text{For } \sigma_y = 33 \text{ ksi}, \left(\frac{L}{r}\right)^2 33 \text{ ksi} = \frac{\pi^2 E}{33{,}000\left(\frac{P_o}{P_y}\right)} \qquad (11a)$$

$$\text{For } \sigma_y = \sigma_{y^*} \neq 33 \text{ ksi}, \left(\frac{L}{r}\right)^2_{\sigma_{y^*}} = \frac{\pi^2 E}{\sigma_{y^*}\left(\frac{P_o}{P_y}\right)} \qquad (11b)$$

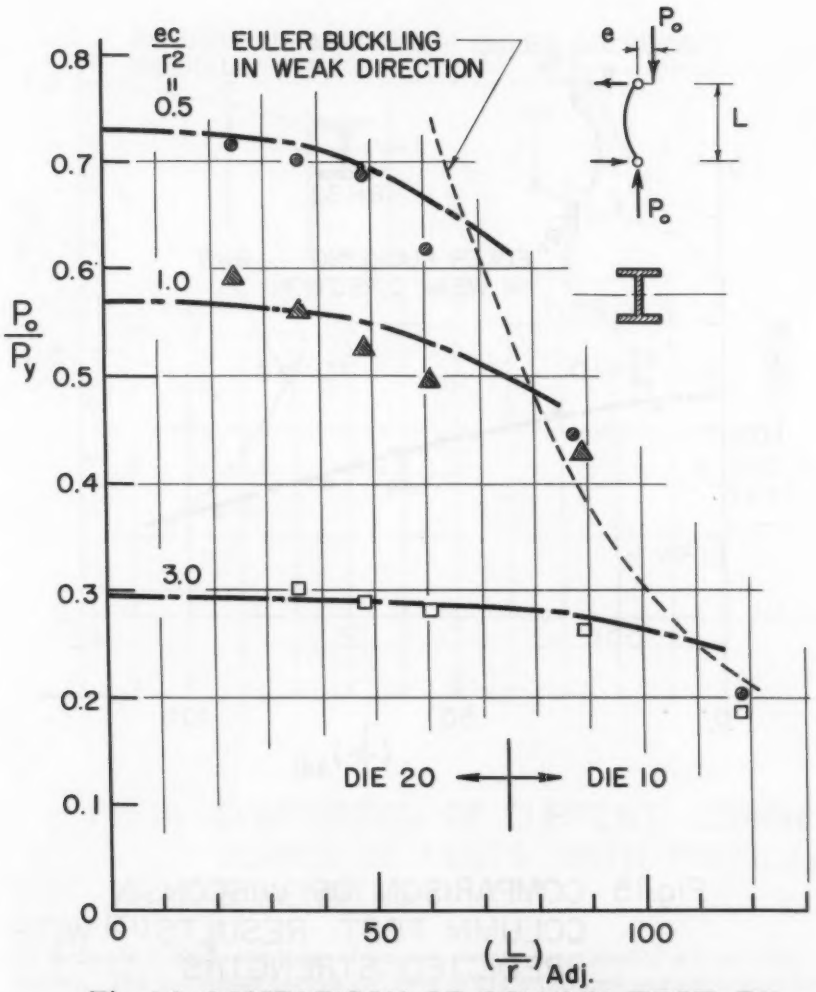

Fig. 14 COMPARISON OF COLUMN TEST RESULTS BY MASSONNET[12] WITH PREDICTED STRENGTHS

Dividing Equation (11a) by Equation (11b) and solving for $\left(\frac{L}{r}\right)$ 33 ksi

$$\left(\frac{L}{r}\right)\sigma_y = 33 \text{ ksi} = \left(\frac{L}{r}\right)\sigma_{y^*}\sqrt{\frac{\sigma_{y^*}}{33{,}000}} \qquad (12)$$

where σ_{y^*} is the yield point stress of the material in question and is given in pounds per square inch.

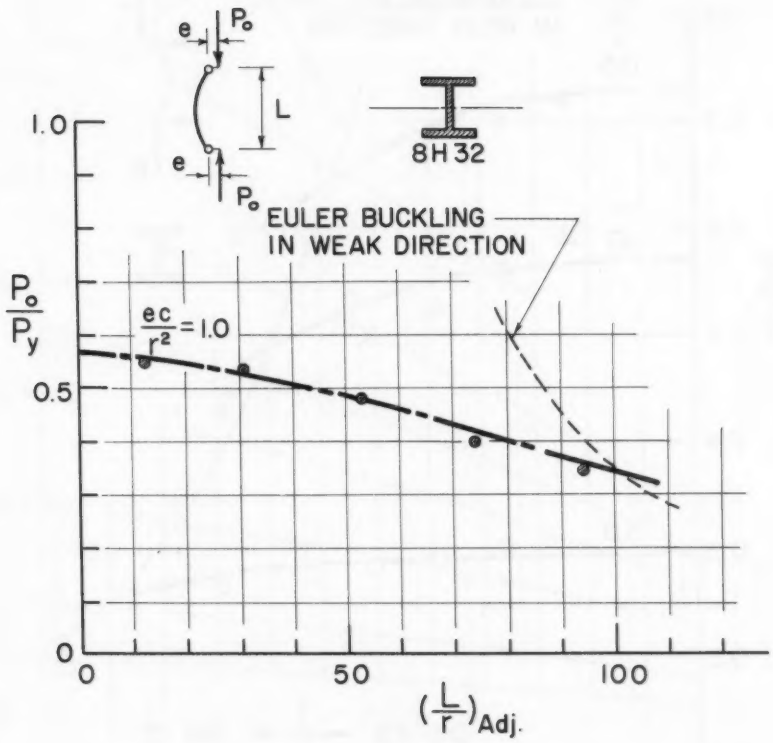

Fig. 15 COMPARISON OF WISCONSIN COLUMN TEST RESULTS[13] WITH PREDICTED STRENGTHS

Equation (12) gives the adjusted slenderness ratio which must be used when comparing test results for a material having a yield point other than 33,000 psi with the predictions of strength given herein. In the following test comparisons the slenderness ratios have been adjusted according to Equation (12). Since the axial thrust and end moment parameters were given in a non-dimensional form involving the yield point stress, it is not necessary to adjust these parameters.

For a majority of the columns that have been tested and are listed herein, the members were subjected to eccentrically applied thrusts. In graphically comparing these test results with the strength predictions of this report slenderness values have been shown as the abscissa and (P_o/P_y) values as

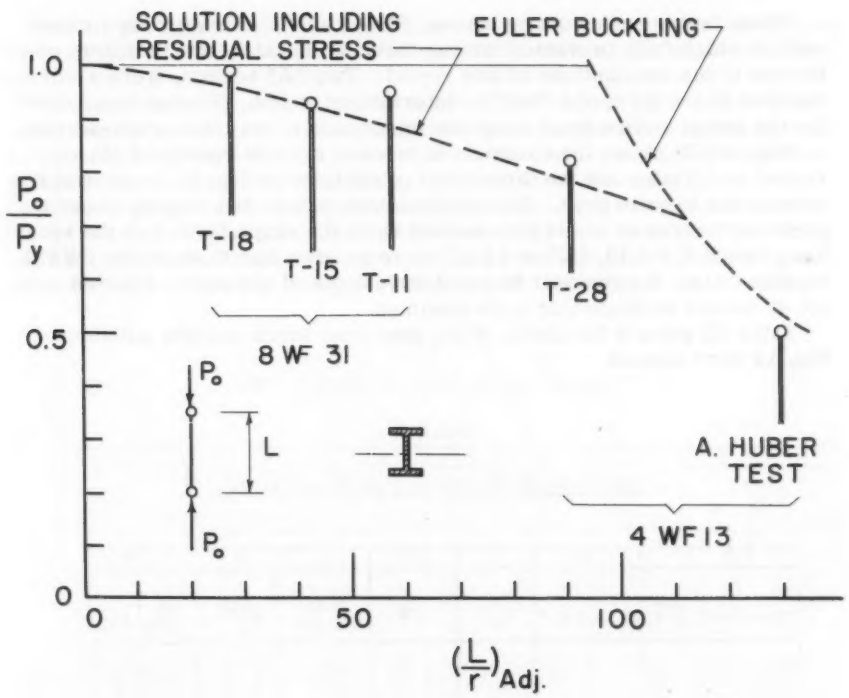

Fig.16 COMPARISON OF CURRENT LEHIGH SERIES OF TESTS WITH PREDICTED STRENGTHS

the ordinate (i.e., in the form of column curves for constant eccentricity ratios). The individual curves for each of the situations were obtained from Figs. 6 and 7 using the ec/r^2 values shown across the top and along the right hand side of the figure. It should be noted that since

$$\frac{ec}{r^2} = \frac{\left[M_o/M_p\right]}{\left[P/P_y\right]} f \qquad (13)$$

and since the values of ec/r^2 given in Figs. 6 and 7 were obtained by using "f" of the 8WF31 shape (one of the lowest shape factors), the theoretical curves should be somewhat conservative for most of the sections tested.

Corness University (Ref. 9)

These tests carried out by Mason, Fisher and Winter were on a cross-section which fully prevented lateral-torsional buckling and therefore conformed to the assumptions of this report. Two "Z" sections were welded together in the form of a "hat" by intermittent welds. Bending was forced (by the use of knife-edges) about the minor axis of the total cross-section.

Figure (12) shows the comparison between the test results of Mason, Fisher and Winter and the theoretical predictions of Fig. 6. In general the correlation is quite good. The experimental results fall slightly above the predicted curves as would be expected since the shape factors of the sections tested (f = 1.18, 1.25 and 1.17) were greater than those of the 8WF31 section. Also, the residual stress distributions of the sections tested were not as severe as those that were assumed.

Table (2) gives a tabulation of the data from which the test points of Fig. 12 were plotted.

TABLE 2

TEST RESULTS OF MASON, FISHER and WINTER [9]

(1) Specimen	(2) Material*	(3) $\left(\frac{L}{r_x}\right)$	(4) $\frac{ec}{r^2}$	(5) P_{ult} (kips)	(6) $\frac{P_{ult}}{P_y}$	(7) $\left(\frac{L}{r_x}\right)_{Adj.}$
1/4 x 3 - 49	1	49	0.25	122	0.73	55.6
1/4 x 3 - 69	1	69	0.25	110	0.66	78.4
1/4 x 3 - 108	1	108	0.25	75	0.45	122.7
1/4 x 3 - 49	1	49	0.75	89.3	0.53	55.6
1/4 x 3 - 69	1	69	0.75	77.6	0.46	78.4
1/4 x 3 - 108	1	108	0.75	57.2	0.34	122.7
1/4 x 3 - 49	1	49	1.50	65.9	0.39	55.6
1/4 x 3 - 69	1	69	1.50	58.4	0.35	78.4
1/4 x 3 - 108	1	108	1.50	43.2	0.26	122.7
1/4 x 4 - 36	2	36	0.25	171.8	0.80	41.8
1/4 x 4 - 66	2	66	0.25	143.8	0.67	76.6
1/4 x 4 - 110.5	2	110.5	0.25	87.8	0.41	128.2
1/4 x 4 - 36	2	36	0.75	123.2	0.58	41.8
1/4 x 4 - 66	2	66	0.75	100.1	0.47	76.6
1/4 x 4 - 110.5	2	110.5	0.75	66.2	0.31	128.2
1/4 x 4 - 36	2	36	1.50	84.2	0.39	41.8
1/4 x 4 - 66	2	66	1.50	71.0	0.33	76.6
1/4 x 4 - 110.5	2	110.5	~ 1.215	58.1	0.27	128.2
1/2 x 3 - 53	3	53	0.25	214.2	0.74	57.6
1/2 x 3 - 74	3	74	0.25	188.6	0.65	80.5
1/2 x 3 - 117	3	117	0.25	122.3	0.42	127.2
1/2 x 3 - 53	3	53	1.50	117.2	0.41	57.6
1/2 x 3 - 74	3	74	1.50	101.2	0.35	80.5
1/2 x 3 - 117	3	117	1.50	76.1	0.26	127.2

* $\sigma_{y(1)}$ = 42.5 ksi, $\sigma_{y(2)}$ = 44.5 ksi, $\sigma_{y(3)}$ = 39.0 ksi

Lehigh University (Ref. 10)

A total of 93 tests were carried out by Johnston and Cheney in this series: 89 were made on 315.7 sections and 6 on 6WF20 sections. A summary of the test data is given in Table (3).

Columns were tested by both concentric and eccentric application of the axial load; however, the column tests under pure axial thrust cannot be compared with the predicted interaction curves. The end-condition of these test specimens were such that they fail by buckling about the weak axis.

In general, the tests were performed on columns which were essentially pin-ended with respect to bending in the strong direction and fixed-ended in the weak direction. This was accomplished by the use of knife-edges placed perpendicular to the web through which the load was applied. The loading

TABLE 3

TEST RESULTS OF JOHNSTON and CHENEY[10]

(1) Test No.	(2) Member	(3) Material*	(4) e (inches)	(5) $\left(\frac{L}{r_x}\right)$	(6) $(\sigma_o)_{max}$ (ksi)	(7) $\frac{ec}{r^2}$ (Approx.)	(8) $\frac{P_o}{P_y}$	(9) $\left(\frac{L}{r_x}\right)_{Adj.}$
C-49	3I5.7	1	1.01	22.6	23.50	1.0	0.56	25.5
C-50	3I5.7	1	1.01	32.6	22.85	1.0	0.54	36.8
C-51	3I5.7	2	1.01	42.1	20.45	1.0	0.50	46.8
C-52	3I5.7	2	1.01	47.1	19.10	1.0	0.47	52.4
C-53	3I5.7	2	1.01	52.1	20.00	1.0	0.49	58.0
C-54	3I5.7	2	1.01	62.0	18.70	1.0	0.46	68.9
C-55	3I5.7	2	1.01	72.0	16.50	1.0	0.40	80.0
C-56	3I5.7	2	1.01	82.0	14.95	1.0	0.37	91.2
C-57	3I5.7	2	1.01	101.8	11.40	1.0	0.28	113.1
C-58	3I5.7	2	1.01	121.6	9.50	1.0	0.23	135.1
C-59	3I5.7	2	0.50	22.3	28.90	0.5	0.71	24.8
C-60	3I5.7	2	1.52	22.3	19.00	1.5	0.47	24.8
C-61	3I5.7	2	2.02	22.3	15.62	2.0	0.38	24.8
C-62	3I5.7	2	3.03	22.3	11.86	3.0	0.29	24.8
C-63	3I5.7	2	5.05	22.3	8.45	5.0	0.21	24.8
C-64	3I5.7	2	7.07	22.3	6.29	7.0	0.15	24.8
C-65	3I5.7	2	0.50	47.1	27.20	0.5	0.67	52.4
C-66	3I5.7	2	1.52	47.1	16.38	1.5	0.40	52.4
C-67	3I5.7	2	2.02	47.1	13.30	2.0	0.33	52.4
C-68	3I5.7	2	3.03	47.1	11.10	3.0	0.27	52.4
C-69	3I5.7	2	5.05	47.1	7.41	5.0	0.18	52.4
C-70	3I5.7	2	7.07	47.1	5.64	7.0	0.14	52.4
C-71	3I5.7	2	0.50	72.0	21.05	0.5	0.52	80.0
C-72	3I5.7	2	1.52	72.0	13.93	1.5	0.34	80.0
C-73	3I5.7	2	2.02	72.0	12.67	2.0	0.31	80.0
C-74	3I5.7	2	3.03	72.0	9.02	3.0	0.22	80.0
C-75	3I5.7	2	5.05	72.0	6.53	5.0	0.16	80.0
C-76	3I5.7	2	7.07	72.0	4.81	7.0	0.12	80.0
6-5	6WF20	3	2.23	46.7	21.6	1.0	0.54	51.2
6-6	6WF20	3	4.45	46.9	14.4	2.0	0.36	51.4

*$\sigma_{y(1)}$ = 42.2 ksi, $\sigma_{y(2)}$ = 40.8 ksi, $\sigma_{y(3)}$ = 39.8 ksi

conditions and support arrangements for the tests correspond to the condition "c" loading of this report (Fig. 6).

As noted in Table 3, the slenderness-ratios were adjusted to account for the yield stress of the material tested. The comparisons between predicted strengths and experimental results are shown in Fig. (13).

Johnston and Cheney report that the "columns loaded eccentrically to produce bending in the strong direction usually failed by plastic lateral torsional buckling" (a condition specifically excluded in this paper). It is interesting to note, however, that except for the tests which fall close to the case where failure would have been due to Euler buckling in the weak direction, the correlation achieved with the developed theory which neglects lateral-torsional behavior is reasonably good.

University of Liege (Ref. 11, 12)

Massonnet reports the results of 95 column tests. The tests were carried out on sections of DIE 10, DIE 20 and PN 22 profiles. Of these, the DIE profiles are geometrically similar to the American wide-flange shape, the shape being considered in this report. Therefore, only the DIE profile tests will be used for comparison. Furthermore, only those tests which correspond to the condition "c" and "d" loading are listed.

The end conditions for Massonnet's test columns were essentially pin-ended in both directions since the end-fixtures consisted of almost frictionless, hydraulically seated steel hemispheres. For such end-conditions, the least possible restraint is provided against lateral torsional buckling.

Table 4 summarizes the applicable test data for the DIE profile tests. Figure (14) gives the comparison between the tests on members subjected to a condition "d" loading and the theoretical predictions shown by the dot-dash curves. As before, the slenderness ratio is adjusted for differences in yield stress level. In all cases the final failure was by lateral torsional buckling; in spite of this, most of the test points agree rather well with the theoretical relationship that neglects this type of failure. It is expected that further theoretical work taking this mode of failure into account will provide a better understanding of the problem and will result in a better correlation in the "transition range."

No comparison has been shown for the condition "c" tests of Ref. 12 (equal and opposite end moments). Due to the condition of loading and end restraints it would be expected that lateral-torsional instability would occur prior to the theoretical load predicted in this paper and this was found to be the case. A solution to the problem of lateral-torsional buckling for this condition of loading which also takes into account the influence of residual stress has just been completed. In general, the correlation is quite good. A report on this latter work will soon be available.

University of Wisconsin (Ref. 13)

The members tested in this investigation were 8H32 shapes, similar to the currently available 8WF31 section. The end-conditions were essentially pin-ended against strong axis bending and fixed in the weak direction. Of the five tests carried-out, the two which had an adjusted slenderness value greater than 50 failed by lateral-torsional buckling at a load slightly less than that predicted.

TABLE 4

TEST RESULTS of MASSONNET (12)

(1) Test No.	(2) Section	(3) Loading Condition	(4) $\frac{ec}{r^2}$	(5) Pmax (tons)	(6) Py (tons)	(7) $\left(\frac{L}{r_x}\right)$	(8) $\frac{P_o}{P_y}$	(9) $\left(\frac{L}{r_x}\right)_{Adj.}$
1	DIE 20 [1]	c	0.5	88.8	132	23.6	0.67	24.1
2	DIE 20	c	1.0	66.8	132	23.7	0.51	24.2
3	DIE 20	c	3.0	35.8	132	23.7	0.27	24.2
8	DIE 20	c	0.5	84.8	134	35.6	0.63	36.3
9	DIE 20	c	1.0	64.8	133	35.4	0.49	36.1
10	DIE 20	c	3.0	32.8	133	35.5	0.25	36.2
16	DIE 20	c	0.5	71.0	135	44.4	0.53	45.3
17	DIE 20	c	1.0	59.0	134	44.2	0.44	45.1
18	DIE 20	c	3.0	32.5	134	44.4	0.24	45.3
24	DIE 20	c	0.5	62.0	134	59.1	0.46	60.4
25	DIE 20	c	1.0	53.5	133	58.7	0.40	60.0
26	DIE 20	c	3.0	29.0	134	59.2	0.22	60.4
33	DIE 10 [2]	c	0.5	22.8	53.8	80.8	0.42	87.0
34	DIE 10	c	1.0	19.3	54.5	82.4	0.35	88.6
35	DIE 10	c	3.0	11.5	55.0	82.6	0.21	89.1
42	DIE 10	c	0.5	13.8	57.1	109.9	0.24	118.2
43	DIE 10	c	1.0	12.4	55.6	110.3	0.22	119.0
44	DIE 10	c	3.0	9.05	55.7	109.6	0.16	118.0
4	DIE 20	d	0.5	95.0	133	23.6	0.72	24.1
5	DIE 20	d	1.0	78.8	133	23.6	0.59	24.2
11	DIE 20	d	0.5	93.8	134	35.6	0.70	36.3
12	DIE 20	d	1.0	74.8	133	35.3	0.56	36.1
13	DIE 20	d	3.0	40.3	133	35.2	0.30	36.0
19	DIE 20	d	0.5	90.8	133	47.4	0.68	48.1
20	DIE 20	d	1.0	70.0	133	47.7	0.53	48.4
21	DIE 20	d	3.0	39.0	134	47.7	0.29	48.4
27	DIE 20	d	0.5	82.0	133	59.0	0.62	60.2
28	DIE 20	d	1.0	67.0	135	59.6	0.50	60.8
29	DIE 20	d	3.0	38.1	135	59.2	0.28	60.4
36	DIE 10	d	0.5	25.0	56.4	81.9	0.44	88.2
37	DIE 10	d	1.0	24.4	56.4	82.7	0.43	89.2
38	DIE 10	d	3.0	15.05	57.0	82.7	0.26	89.2
45	DIE 10	d	0.5	11.8	57.7	109.1	0.20	117.8
47	DIE 10	d	3.0	10.8	57.7	109.1	0.19	117.8

(1) σ_y = 34.2 ksi (2) σ_y = 38.2 ksi

Lehigh University (Ref. 2, 6, 16)

Table (6) summarizes the results of the tests in this series that are applicable. Since the majority of the members were tested in a range where the interaction curves converge to a point (i.e., for low values of P_o/P_y) most of these have not been shown on graphs. For the pure axial load tests, however, Fig. 16 shows the correlation with predicted strength. An additional test by Huber(14) (4WF13, $L/_r$=130) has been included to extend the range of coverage.

TABLE 5

TEST RESULTS of WISCONSIN SERIES[13]

(1)	(2)	(3)	(4)	(5)	(6)	(7)	(8)
Test No.	Member	$\frac{ec}{r^2}$	$\left(\frac{L}{r_x}\right)$	σ_{ult} (ksi)	σ_y (ksi)	$\frac{P_o}{P_y}$	$\left(\frac{L}{r_x}\right)$ Adj.
H-1	8H32 [1]	1.00	11.4	20.7	37.4	0.55	12.1
H-2	8H32 [1]	1.00	29.0	19.95	37.4	0.53	30.9
H-3	8H32 [1]	1.00	49.5	17.95	37.4	0.48	52.7
H-4	8H32 [2]	1.00	69.6	15.10	38.0	0.40	74.6
H-5	8H32 [3]	1.00	89.7	12.60	36.4	0.35	94.2

(1) σ_y = 37.4 ksi

(2) σ_y = 38.0 ksi

(3) σ_y = 36.4 ksi

V. DISCUSSION AND SUMMARY

For the conditions of end restraint and the loading conditions of Fig. 1, solutions to the problem of the determination of the maximum carrying capacity of wide flange shapes loading in the plane of the web have been presented. These solutions assume that the member in question will fail by excessive bending in the plane of the applied moment. Failure due to lateral-torsional or local buckling has not been considered. The resulting interaction curves (Figs. 6 and 7) do, however, include the influence of a typical cooling type residual stress pattern.

Approximate interaction equations, which cover the range most often encountered in practice, were developed to eliminate the need for interpolation (Equations 5 and 7).

Currently available test results were compared against the strength predictions of Figs. 6 and 7. The tests carried-out by Mason, Fisher and Winter were the only ones that directly fulfill the assumptions of this report and the correlation was shown to be very good (Fig. 12). For the cases where the members tested were pin-ended in the strong direction and fixed in the weak, the curves give reasonably reliable results provided Euler buckling in the weak direction was not imminent (Figs. 13, 15 and 16). Where the members were pin-ended in both directions, lateral-torsional buckling was a major factor in determining strength (Fig. 14). The test results corresponding to this situation (Massonnet) seem to indicate that for a condition "d" type of loading the overall behavior can still be approximated by the curves of Fig. (7) but with less accuracy than in the aforementioned cases (Fig. 14). Members loaded in a condition "c" manner, however, carry markedly less load than predicted.

TABLE 6

TEST RESULTS OF THE CURRENT LEHIGH TEST SERIES

(1)	(2)	(3)	(4)	(5)	(6)	(7)	(8)
Test No.	Member	Loading Condition	Experimental* σ_y = 40 ksi + P_a/P_y	Experimental* σ_y = 40 ksi + M_o/M_p	Experimental* Adjusted σ_y # P_a/P_y	Experimental* Adjusted σ_y # M_o/M_p	$\left(\frac{L}{r_x}\right)_{Adj.}$
T-8	8WF31	c	0.62	0.12	0.68	0.13	58
T-11	8WF31	c	0.87	0	0.95	0	58
T-12	8WF31	c	0.12	0.84	0.13	0.92	58
T-15	8WF31	c	0.85	0	0.93	0	43
T-16	8WF31	c	0.12	0.78	0.13	0.85	43
T-18	8WF31	c	0.91	0	0.99	0	28
T-19	8WF31	c	0.12	0.81	0.13	0.88	28
T-20	4WF13	c	0.12	0.84	0.12	0.87	60
T-26	4WF13	c	0.12	0.79	0.12	0.81	91
T-28	4WF13	c	0.80	0	0.82	0	91
T-32	4WF13	c	0.12	0.76	0.12	0.78	120
T-13	8WF31	d	0.12	1.05	0.13	1.14	58
T-23	4WF13	d	0.12	1.05	0.12	1.08	91
T-31	4WF13	d	0.12	0.98	0.12	1.01	120

* Parameters that were held constant are underlined.

+ σ_y = 40 ksi determined from tension coupon tests.

\# Adjusted σ_y (to take into account the influence of strain rate) was obtained by pro-rating the tension coupon value in the same ratios as those given in Ref. 15. (Note: values change for different sections.)

Further work is currently underway to include the influence of lateral-torsional instability into the strength calculations and preliminary results of this study indicate that good correlation can be achieved when this type of failure is considered.

VI. ACKNOWLEDGMENTS

This study was part of the general investigation "Welded Continuous Frames and Their Components" currently being carried-out at Fritz Engineering Laboratory, Lehigh University under the general direction of Lynn S. Beedle. The investigation is sponsored jointly by the Welding Research Council and the Department of the Navy with funds furnished by the American Iron and Steel Institute, American Institute of Steel Construction, Office of Naval Research, Bureau of Ships and Bureau of Yards and Docks.

William J. Eney is Director of Fritz Engineering Laboratory and Head of the Department of Civil Engineering.

VII. REFERENCES

1. Beedle, L. S., Thürlimann, B., and Ketter, R. L., "PLASTIC DESIGN IN STRUCTURAL STEEL-LECTURE NOTES," AISC and Lehigh University, September 1955.

2. Ketter, R. L., Kaminsky, E. L., and Beedle, L. S., "PLASTIC DEFORMATION OF WIDE-FLANGE BEAM COLUMNS," Transactions of the ASCE, Vol. 120, 1955, p. 1028.

3. Ketter, R. L., "THE INFLUENCE OF RESIDUAL STRESS ON THE STRENGTH OF STRUCTURAL MEMBERS," Proceedings of the 7th Technical Session of the Column Research Council, May 1957.

4. Newmark, N. M., "NUMERICAL PROCEDURES FOR COMPUTING DEFLECTIONS, MOMENTS AND BUCKLING LOADS," Transactions of the ASCE, Vol. 108, 1943, p. 1161.

5. Timoshenko, S., "THEORY OF ELASTIC STABILITY," McGraw-Hill Book Co., New York, 1939.

6. Ketter, R. L., Beedle, L. S., and Johnston, B. G., "COLUMN STRENGTH UNDER COMBINED BENDING AND THRUST," The Welding Journal 31(12), Research Supplement, 607-s to 662-s 1952.

7. Galambos, T. V., and Ketter, R. L., "FURTHER STUDIES OF COLUMNS UNDER COMBINED BENDING AND THRUST," Fritz Engineering Laboratory Report No. 205A.19, June 1957.

8. A Report of Research Committee E of Column Research Council "SOME RECOMMENDATIONS RELATING TO DESIGN SPECIFICATIONS FOR STEEL BEAMS AND MEMBERS SUBJECTED TO COMPRESSION AND BENDING," May 1954.

9. Mason, R. E., Fisher, G. P., and Winter, G., "TESTS AND ANALYSIS OF ECCENTRICALLY LOADED COLUMNS," Dept. of Structural Eng., School of Eng., Cornell Univ., Ithaca, New York, April 1956.

10. Johnston, B. G., and Cheney, L., "STEEL COLUMNS OF ROLLED WIDE FLANGE SECTION," Progress Report No. 2, American Institute of Steel Construction, November 1942.

11. Massonnet, C., and Campus, F., "CORRESPONDENCE ON THE 'STAUCHION PROBLEM IN FRAME STRUCTURES DESIGNED ACCORDING TO ULTIMATE CARRYING CAPACITY' by Horne, M. R.," Proc. Inst. of Civil Engrs. par III, Vol. 5, p. 558-571, August 1956.

12. Massonnet, C., and Campus, F., "RECHERCHES SUR LE FLAMBENTENT DE COLONNES EN ACIER A 37, A PROFIL EN DOUBLE TE, SOLLICITEES OBLIQUEMENT," I.R.S.I.A. Bulletin No. 17, April 1956.

13. "SECOND PROGRESS REPORT OF THE SPECIAL COMMITTEE ON STEEL COLUMNS" Paper No. 1789, ASCE Transactions, Vol. 95, 1931.

14. Huber, A. W., "THE INFLUENCE OF RESIDUAL STRESS ON THE INSTABILITY OF COLUMNS," Lehigh University Dissertation, May 1956.

15. Gozum, A. T., and Huber, A. W., "MATERIAL PROPERTIES, RESIDUAL STRESSES AND COLUMN STRENGTH," Fritz Engineering Report No. 220A.14, May 1955 (Revised November 1955)

16. Beedle, L. S., Ready, J. A., and Johnston, B. G., "TESTS OF COLUMNS UNDER COMBINED THRUST AND MOMENT," Proceeding, Society for Experimental Stress Analysis VIII, No. 1, 109 (1950).

17. Bijlaard, P. P., Fisher, G. D., Winter, G., "ECCENTRICALLY LOADED, END-RESTRAINED COLUMNS" Transactions of the ASCE, Vol. 120, 1955 p. 1070.

18. Shanley, F. R., "APPLIED COLUMN THEORY" Transactions of the ASCE, Vol. 115, 1950, p. 698.

VIII. Nomenclature

A	Area of cross-section (in^2)
B,G,J,K	Non-dimensional constants
E	Young's Modulus of Elasticity (E=30,000,000 psi for A7 steel)
I	Moment of Inertia (in^4)
L	Length of member (inches)
M	Bending of Moment (inch-kips)
M_o	Applied moment at the end of the member
$M_p=Z\sigma_y$	Fully plastic moment value under pure moment
$M_y=S\sigma_y$	Initial yield moment value under pure moment
P	Axial thrust (kips)
P_o	Axial thrust at maximum load capacity for beam-columns
$P_y=A\sigma_y$	Axial load corresponding to compressive yield stress over entire section
S	Section modulus about the strong axis (in^3)
Z	Plastic modulus about the strong axis (in^3)
f	Shape factor ($f = \frac{M_p}{M_y} = \frac{Z}{S}$)
b	Flange width
c	Distance from centroid to outer fiber
d	Depth of section
e	Eccentricity (inches)
$k=\sqrt{P/EI}$	
r	Radius of gyration about the strong axis
t	Thickness of flange
w	Thickness of web

x	Distance along the axis of a member, as shown on Fig. 1
y	Deflection (inches)
$\frac{ec}{r^2}$	Eccentricity ratio
$L/_r$	Slenderness ratio
$\alpha,$	Non-dimensional constants
$\xi = \frac{\sigma_y}{\pi^2 E}$	Constant defining properties of material
δ	Deflection at specific station along the member (inches)
θ	End rotation (radians)
ϕ	Curvature (radians/inch)
$\phi_y = \frac{2\sigma_y}{Ed}$	Curvature corresponding to initial yield under pure moment
λ	Length of equally spaced segments of total member length
ϵ	Strain (inches/inch)
ϵ_y	Strain corresponding to initial yield point stress
σ	Stress (lbs/inch^2)
σ_y	Yield stress (assumed to be 33 ksi for A7 steel)

Journal of the
ENGINEERING MECHANICS DIVISION
Proceedings of the American Society of Civil Engineers

SEEPAGE LOSSES FROM IRRIGATION CANALS

H. Y. Hammad[1]

ABSTRACT

This paper deals with the two-dimensional problem of steady seepage flow under gravity from a canal into a semi-pervious clay layer of finite thickness underlain by a freely permeable layer of sand and gravel in which the piezometric head is very near the canal water level. Two steps of conformal mapping are used and an approximation to the canal profile is adopted. In this approximation the specified canal width and depth are untouched.

INTRODUCTION

In many agricultural zones, especially in river valleys, the stratified soil is formed of a top clay layer of finite thickness and medium or low permeability, underlain by highly permeable layers of sand and gravel. The piezometric head in the lower freely permeable layers is controlled by the powerful river running in the valley. For irrigation purposes, canals running in the top clay layer are usually run at higher water level than the piezometric level in the lower sand and gravel. Consequently a continuous steady seepage flow takes place from the canal through the clay layer to the sand and gravel layers.

In the present treatment the piezometric level in the lower sand and gravel layers is considered very near the canal water level. This case is met with in places with high ground water-table. The same problem, but with very deep lying water-table in the lower sand and gravel layer has been solved in 1934 by V. V. Wedernikow.(1)

Governing Equations and Boundary Conditions

As may be found in texts on flow through porous media,(1) the governing

Note: Discussion open until September 1, 1959. To extend the closing date one month, a written request must be filed with the Executive Secretary, ASCE. Paper 1991 is part of the copyrighted Journal of the Engineering Mechanics Division, Proceedings of the American Society of Civil Engineers, Vol. 85, No. EM 2, April, 1959.

1. Asst. Prof. of Applied Mechanics, Faculty of Eng., Alexandria Univ., Alexandria, Egypt.

differential equation of the flow is that of Laplace, viz:

$$\nabla^2 \phi = \frac{\partial^2 \phi}{\partial x^2} + \frac{\partial^2 \phi}{\partial y^2} = 0 \quad , \tag{1}$$

to be satisfied everywhere in the field of motion, ϕ being the velocity-potential given by

$$\phi = \bar{k} \left(\frac{p}{\rho g} - y \right) + C \quad , \tag{2}$$

where $\bar{k}$ is the permeability of the porous medium, p is the pressure at any point, ρ is the fluid density and g is the acceleration due to gravity.

According to the above assumptions, the boundary conditions are:

1. The line of separation between the semi-pervious clay strip and the lower freely permeable layer of sand and gravel is an equipotential line.
2. The canal profile is also an equipotential line.
3. The pressure vanishes on the free water surface which is also a stream-line.
4. The rise of water by capillarity from the free water surface is neglected.

Method of Solution

A first order solution of the problem of seepage from a shallow canal (depth d < semi-breadth B) may be obtained by considering the seepage under gravity through an aperture ($-b < x < +b$) in the solid boundary $y = o$, into the semi-pervious strip bounded by $y = o$ and $y = D$ in the Z- plane as shown in figure. The line segment ($y = o$, $-b < x < +b$) is an equipotential, while ($y = o$, $b < x < \infty$) and ($y = o$, $-\infty < x < -b$) are stream-lines. The line $y = D$ is an equipotential.

It has been already assumed that the free water surface in the seepage layer is high and very near the canal water level. Consequently, for a first order approximate solution, the line segments ($y = o$, $b < x < \infty$) and ($y = o$, $-\infty < x < -b$) have been taken as the top stream-lines instead of the real free surface which is very near to them, as our original assumption.

The complex-potential $w (= \phi + i\psi)$ of the flow may be obtained by two steps of conformal transformation using the Schwarz-Christoffel theorem in each step, ϕ being the velocity-potential, ψ the stream-function and $i = \sqrt{-1}$ in the usual notation:

1. Mapping conformally the infinite strip bounded by $y = o$ and $y = D$ in the Z=plane onto the lower half of the ζ-plane (see figure) we get in terms of complex functions:

$$\frac{dz}{d\zeta} = \frac{A}{(1-\zeta)(1+\zeta)} \quad , \tag{3}$$

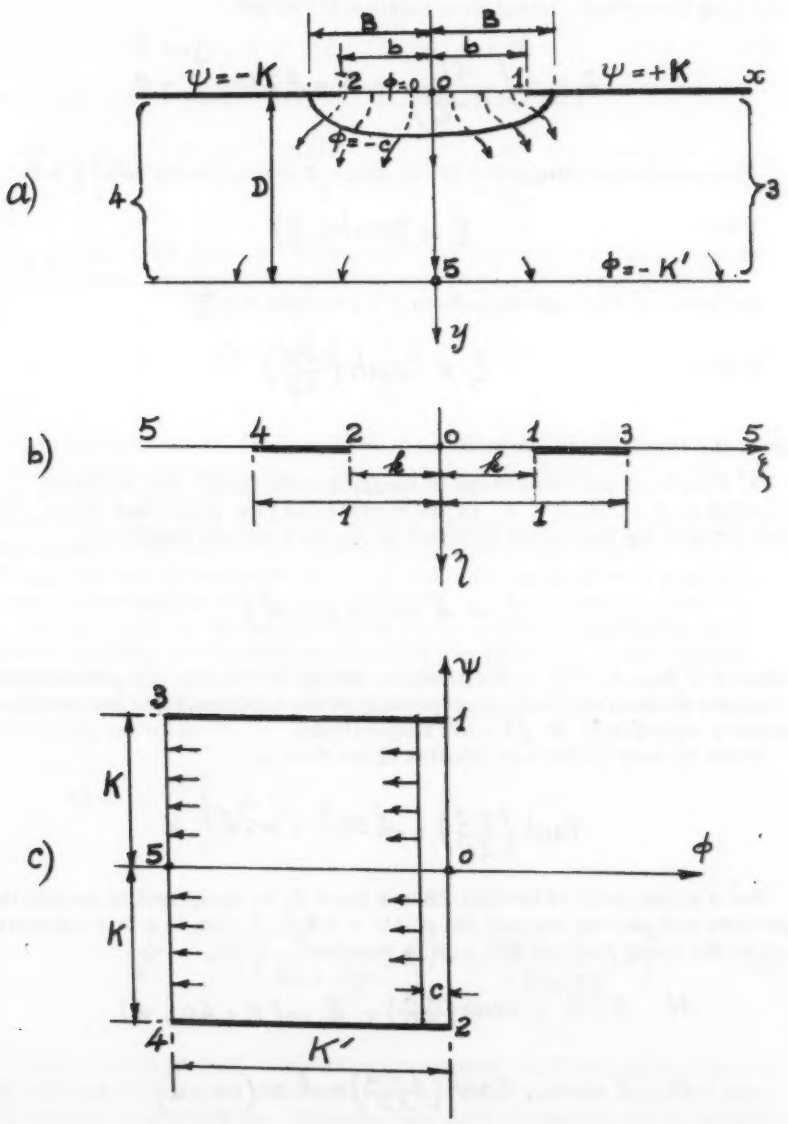

Fig. 1: Steps of Conformal Mapping.
a) z-plane, b) ζ-plane, c) w-plane.

the points having the same numbers in both planes correspond to one another and A is a constant. Integrating relation (3) we get

$$Z = A\int \frac{d\zeta}{(1-\zeta^2)} + B = A \tanh^{-1}\zeta + B \qquad (4)$$

The constant of integration B = o, since Z = o corresponds to ζ = o.

Hence $$\zeta = \tanh\left(\frac{Z}{A}\right) \qquad (5)$$

But since Z = iD corresponds to $\zeta = i\infty$, than $A = \frac{2D}{\pi}$

Hence $$\zeta = \tanh\left(\frac{\pi Z}{2D}\right) \qquad (6)$$

gives the required transformation.

2. Following the same steps in mapping conformally the rectangle bounded by $\psi = \pm K$, $\phi = -K'$ in the w-plane onto the lower half of the ζ-plane (see figure), we finally get in terms of Jacobi's elliptic functions:

$$\zeta = k\, sn(-iw, k) \qquad (7)$$

where k (= tank πb/2D) is the modulus, and K, K' are the complete elliptic integrals of the first kind corresponding to the modulus k and the complementary modulus k' (= $\sqrt{1 - k^2}$) respectively.

From (6) and (7) the w-z relation of the flow is

$$\tanh\left(\frac{\pi Z}{2D}\right) = k\, sn(-iw, k) \qquad (8)$$

For a given canal of breadth 2B and depth d, an equipotential around the aperture and passing through the points $Z = \pm B$, Z = id, is a fair approximation to the canal profiles met with in practice.

$$At \quad Z = B \;,\; \tanh\left(\frac{\pi B}{2D}\right) = k\, sn(K + ic, k) \qquad (9)$$

$$At \quad Z = id \;,\; \tanh\left(\frac{i\pi d}{2D}\right) = k\, sn(ic, k) \qquad (10)$$

where -c is the potential along the canal profile. For a specified breadth 2B and depth d of the canal, equations (9) and (10) give the two unknowns c and k, where k = tanh (π^b/2D). In other words the breadth and depth of the canal will define the appropriate breadth of the aperture 2b and the constant potential value to be assessed to the canal profile. Let B' = tanh (πB/2D) and d' = tan (πd/2D). Equations (9) and (10) reduce to

$$k / dn(c, k') = B' \tag{11}$$

$$k\, sn(c, k') / cn(c, k') = d' \tag{12}$$

For small (d/D), equations (11) and (12) give on solution

$$k = \frac{1}{2}\left[B' + \sqrt{B'^2 - 2d'^2}\right] \quad , \quad c = 2d' \Big/ \left[B' + \sqrt{B'^2 - 2d'^2}\right] \tag{13}$$

From an argument given by Terzaghi,[2] the seepage flux out of each unit length of the canal normal to the plane of motion is accordingly given by

$$Q = \bar{k} h \cdot \frac{2K}{K' - c} \quad , \tag{14}$$

where h is the head loss between the canal boundary and the line y = D or the difference between the water level in the canal and the free water surface in the soil at great distances from it.

The seepage flux given by (14) is slightly exaggerated by a small amount corresponding to the flow in the narrow strip between the real free surface and the approximated free surface (y = o) which is assumed very near to it.

It may be worthwhile mentioning that in the case of a drain in which the water level is lower by an amount h than the piezometric head in the sand and gravel aquifer, the flux will be reversed and the drain will be gaining water at the rate given by (14) instead of loosing.

From relations (2) and (8), the equation of the free water surface may be approximately given by

$$y = -\frac{\phi}{\bar{k}}\Big]_{y=0} + C$$

$$= \frac{1}{k}\left[dn^{-1}\left(\frac{k}{\tanh \frac{\pi x}{2D}}, k'\right) - dn^{-1}\left(\frac{k}{\tanh \frac{\pi B}{2D}}, k'\right)\right] \tag{15}$$

For deep canals (d > B), a similar approximate solution may be obtained by considering the flow out of an aperture in a solid vertical boundary coinciding with the y-axis and the remaining boundary conditions are as before.

For small canals of nearly semi-circular profile, a point source solution may be adopted.[3]

Numerical Example

Take a canal of depth d = 5 ft. and breadth 2B = 60 ft. running in a clay

layer of thickness D = 50 ft. and permeability $\bar{k}$ = 0.3 ft/day at a level h = 3 ft higher than the piezometric head in the sand and gravel aquifer.

$$d' = \tan\ (\pi d/2D) = \tan\ (\frac{\pi \times 5}{2 \times 50}) = .158$$

$$B' = \tanh\ (\pi B/2D) = \tanh\ (\frac{\pi \times 30}{2 \times 50}) = .735$$

Substituting in relations (13) we get:

the modulus of the elliptic integral k = 0.717, and the potential along the canal profile -c = -.220.

From tables of elliptic functions,[4] the complete elliptic integral of modulus k = 0.717 is K = 1.860. For the complementary modulus $k' = v\ (1 = k^2)$ = 0.695, the complete elliptic integral K' = 1.835.

Hence the seepage loss per unit length of canal as given by (14) is

Q = 2.08 ft^3/day/ft length of canal
= 0.011 gal./min./ft length of canal.

BIBLIOGRAPHY

1. Muskat M., Flow of Homogeneous Fluids through Porous Media. J. W. Edwards 1946.
2. Terzaghi K., Theoretical Soil Mechanics. John Wiley & Sons N. Y. 1946, pp. 246 & 247.
3. Hammad H. Y., Behaviour of Subsoil Water-table under a System of Covered Drains. Proc. Second International Congress on Irrigation & Drainage 1954.
4. Dale J. B., Five Figure Tables of Mathematical Functions, Edward Arnold & Co., London, 1949.

Journal of the
ENGINEERING MECHANICS DIVISION
Proceedings of the American Society of Civil Engineers

TORQUE-LOADED CONTINUOUS BEAMS OF PROFILE SECTION

D. H. Young[1] and J. F. Brahtz,[2] M. ASCE

SYNOPSIS

If a beam of thin profile section is continuous over several supports and subjected to transverse loads not on the shear-center axis, it will undergo torsion as well as bending. Beginning with the general theory of non-uniform torsion for such bars, expressions for the angle of twist ϕ along the bar are written for two consecutive spans. From these expressions, a single recurrence type formula is derived which involves, as unknowns, only the three quantities $\phi''_n, \phi''_{n+1}, \phi''_{n+2}$, at three consecutive supports. This recurrence formula is somewhat analogous to the three-moment equation and greatly simplifies the analysis of the torsional behavior of a continuous beam subjected to eccentrically applied transverse loads. Its application to the case of a two-span beam is illustrated by an example and an experimental study of this two-span case is described. The results of this experiment are in very good agreement with the theory.

Theory

Consider, in Fig. 1, the case of a continuous beam of thin-walled open profile section subjected to the action of various transverse loads. Each load can be replaced by a parallel load applied on the shear-center axis z and a torque. The loads on the shear-center axis produce only bending and the corresponding stresses and deflections can be found without difficulty from the theory of bending of continuous beams. The main purpose of this paper is to develop a general method of finding the stresses and deformations produced by the torques. This can be done by using the general theory of non-uniform torsion of bars of thin walled open section as developed by

Note: Discussion open until September 1, 1959. To extend the closing date one month, a written request must be filed with the Executive Secretary, ASCE. Paper 1992 is part of the copyrighted Journal of the Engineering Mechanics Division, Proceedings of the American Society of Civil Engineers, Vol. 85, No. EM 2, April, 1959.

1. Prof. of Civ. Engr., Stanford Univ., Stanford, Calif.
2. Director of Engr., J. H. Pomeroy & Co., Los Angeles, Cal.

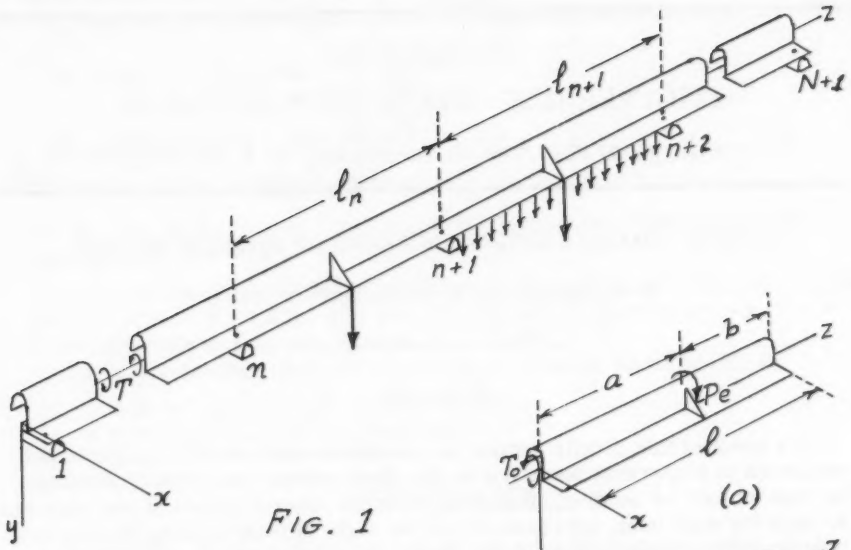

FIG. 1

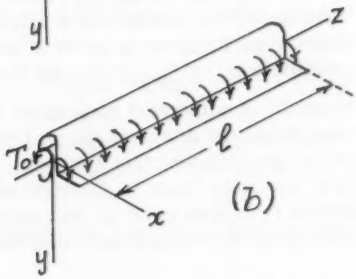

FIG. 2

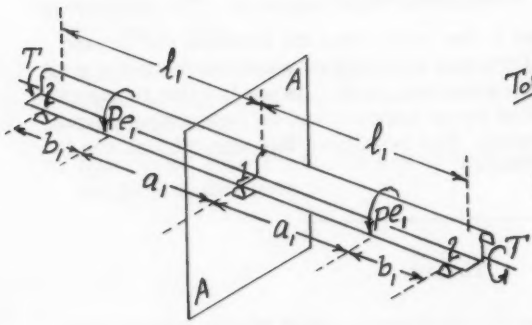

FIG. 3

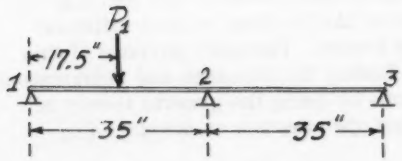

FIG. 4

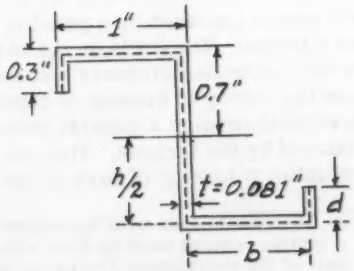

FIG. 5

Timoshenko,[1] Wagner,[4] and others. Such treatment will be much simplified if the effect of bending stresses σ_z on the torsional rigidity of the bar is neglected.[2,3] Then the differential equation governing the relation between torque T and angle of twist ϕ along the bar is

$$T = C\phi' - C_1\phi''' \tag{1}$$

wherein the primes denote differentiation with respect to z. The torque T is considered positive as shown in Fig. 1 and C, C_1, respectively, are the torsional rigidity and warping rigidity constants for the cross-section (1).

Consider now any single span, Fig. 2, having a concentrated torque Pe applied at the distance z = a from the left end. Then for $0 \leq z \leq a$, the torque T is constant and equal to the torque T_o just to the right side of the left-hand support. For such case, the solution of Eq. (1) becomes

$$\phi = \frac{T_o z}{C} + A + A_1 \sinh kz + A_2 \cosh kz$$

where $k^2 = C/C_1$ and A, A_1, A_2 are constants of integration. For z = 0, this solution gives

$$\phi_o = A + A_2, \qquad \phi_o' = \frac{T_o}{C} + kA_1, \qquad \phi_o'' = k^2 A_2 .$$

When these expressions are solved for A, A_1, A_2, in terms of ϕ_o, ϕ_o', ϕ_o'', and these values substituted back into the general solution, it becomes,

$$\phi = \phi_o + \frac{\phi_o'}{k} \sinh kz + \frac{\phi_o''}{k^2}(\cosh kz - 1) - \frac{T_o}{kC}(\sinh kz - kz) \tag{2}$$

which expresses the angle of twist ϕ at any cross-section z in terms of the initial values of the quantities ϕ_o, ϕ_o', ϕ_o'', T_o.

For $a \leq z \leq \ell$, the general expression for ϕ can be obtained by superimposing on the solution (2) a term to account for the effect of the applied torque Pe beyond z = a. This effect is given by the last term of Eq. (2) if T_o is replaced by -Pe and z by z-a. Hence for values of z greater than a,

$$\phi = \phi_o + \frac{\phi_o'}{k} \sinh kz + \frac{\phi_o''}{k^2}(\cosh kz - 1) - \frac{T_o}{kC}(\sinh kz - kz) + \frac{Pe}{kC}\left[\sinh k(z-a) - k(z-a)\right] \tag{3}$$

Equations (2) and (3) represent the complete solution for the case of a single span subjected to a concentrated torque Pe at some intermediate cross-section.

If, instead of a concentrated load P, a single span is subjected to uniformly distributed load of intensity q applied with eccentricity e, Fig. 2b, the torque $T = T_o - qez$, where atain T_o is the torque at the left end of the span taken as

the origin of z. With this value of T, integration of Eq. (1) gives

$$\phi = \phi_o + \frac{\phi'_o}{k}\sinh kz + \frac{\phi''_o}{k^2}(\cosh kz - 1) - \frac{T_o}{kC}(\sinh kz - kz) + \frac{qe}{k^2C}(\cosh kz - \frac{(kz)^2}{2} - 1) \tag{4}$$

Consider now any span ℓ_n of the continuous beam in Fig. 1 where it is assumed that all supports are on the same level and offer no more constraint than to prevent x- and y-displacements as well as rotation about the z-axis of the supported cross-section. Then at the ends of this span, $\phi_n = \phi_{n+1} = 0$. Substitution of these end conditions together with $z = \ell_n$ into Eq. (3) and its derivatives ϕ' and ϕ'' gives, for the case of a single concentrated torque $(Pe)_n$ on the span,

$$\left.\begin{aligned} 0 &= \frac{\phi'_n}{k}\sinh k\ell_n + \frac{\phi''_n}{k^2}(\cosh k\ell_n - 1) - \frac{T_n}{kC}(\sinh k\ell_n - k\ell_n) + \frac{(Pe)_n}{kC}(\sinh kb_n - kb_n), \\ \phi'_{n+1} &= \phi'_n \cosh k\ell_n + \frac{\phi''_n}{k}\sinh k\ell_n - \frac{T_n}{C}(\cosh k\ell_n - 1) + \frac{(Pe)_n}{C}(\cosh kb_n - 1), \\ \phi''_{n+1} &= \phi'_n k \sinh k\ell_n + \phi''_n \cosh k\ell_n - \frac{kT_n}{C}\sinh k\ell_n + \frac{k(Pe)_n}{C}\sinh kb_n. \end{aligned}\right\} \tag{5}$$

Elimination of ϕ'_n between the first and third of these equations yields

$$T_n = (\phi''_n - \phi''_{n+1})\frac{C_1}{\ell_n} + \frac{(Pe)_n b_n}{\ell_n} . \tag{6a}$$

This equation expresses the torque T_n just to the right of the support n in terms of ϕ''_n and ϕ''_{n+1} at the two ends of the span ℓ_n and the applied torque load $(Pe)_n$. There is one such equation for each span of the continuous beam. Thus when all the values $\phi''_1, \phi''_2, \ldots \phi''_{N+1}$ are known, the internal torques $T_1, T_2, \ldots T_N$, just to the right of each support, can be computed from Eq. (6a) and the problem is solved.

To find a relationship between three consecutive values $\phi''_n, \phi''_{n+1}, \phi''_{n+2}$, at three supports, Eq. (3) can also be applied to the span ℓ_{n+1}. This will give another set of three equations similar to Eqs. (5) above, except that the subscript n becomes n+1 while the subscript n+1 becomes n+2. These six equations for two consecutive spans contain eight unknowns, namely, $\phi''_n, \phi''_{n+1}, \phi''_{n+2}, \phi'_n, \phi'_{n+1}, \phi'_{n+2}$, T_n, and T_{n+1}. Although tedious, it is possible to

eliminate from these six equations the five unknowns $\phi'_n, \phi'_{n+1}, \phi'_{n+2}, T_n, T_{n+1}$. This leaves the following equation expressing the desired relationship between ϕ''_n, ϕ''_{n+1}, and ϕ''_{n+2} at three supports:

$$\left[\xi(k\ell_n)\right]\phi''_n + \left[\eta(k\ell_n) + \eta(k\ell_{n+1})\right]\phi''_{n+1} + \left[\xi(k\ell_{n+1})\right]\phi''_{n+2} = \left[\psi\left(\frac{a_n}{\ell_n},\ k\ell_n\right)\right]\frac{k(Pe)_n}{C} + \left[\psi\left(\frac{b_{n+1}}{\ell_{n+1}},\ k\ell_{n+1}\right)\right]\frac{k(Pe)_{n+1}}{C} \tag{7a}$$

where the functions ξ, η, ψ, depend only on the physical dimensions of the beam and the placement of the loads. These functions are defined as follows:

$$\left.\begin{aligned} \xi(k\ell) &= \frac{1}{k\ell} - \frac{1}{\sinh k\ell} \\ \eta(k\ell) &= \frac{1}{\tanh k\ell} - \frac{1}{k\ell} \\ \psi\left(\frac{a}{\ell},\ k\ell\right) &= \frac{a}{\ell} - \frac{\sinh ka}{\sinh k\ell} \end{aligned}\right\} \tag{8a}$$

Equation (7a) is a recurrence type formula which may be written once for each pair of consecutive spans throughout the continuous beam. Thus its application to a beam subjected to various applied torque loads is somewhat analogous to that of the well known Three Moment Equation used in the analysis of continuous beams subjected to bending loads. In the case of a beam on N+1 supports and having N spans, Eq. (7a) can be written N-1 times. This gives a system of N-1 linear equations involving the N+1 unknowns $\phi''_1, \phi''_2, \ldots\ldots\phi''_{N+1}$. If the cross-sections at the two extreme ends of the beam are free to warp, $\phi''_1 = \phi''_{N+1} = 0$ and Eqs. (7a) are sufficient to determine $\phi''_2, \phi''_3, \ldots\ldots\phi''_N$. As soon as these values are known, the internal torques $T_1, T_2, \ldots\ldots T_N$ can be found from Eq. (6a) and the problem is solved.

If the extreme left end of the beam is built-in so that warping of that cross-section is prevented, the value of ϕ''_1 is not known but instead, as a condition of constraint against warping, $\phi'_1 = 0$. The simplest way to handle this situation is as follows: Imagine a mirror at the built-in end which reflects the span ℓ_1 and its torque load $(Pe)_1$ as shown in Fig. 3. Then the reflected span ℓ_1 and the actual span ℓ_1 represent two consecutive spans for which the plane AA is a plane of symmetry. From this it follows that the condition $\phi'_1 = 0$ will be satisfied. Hence Eq. (7a) may be written for these two consecutive spans yielding an additional equation to match the additional unknown ϕ''_1. In applying Eq. (7a) to the fictitious situation in Fig. 3, it must be noted that b_1 should be substituted for both a_n and b_{n+1}, while ℓ_1 is substituted for both ℓ_n and ℓ_{n+1}. The same procedure may be used if the extreme right end of the beam is built-in.

The previous discussion has treated only the case of a continuous beam subjected to eccentrically applied concentrated forces. The case of uniformly distributed load of intensity q applied with eccentricity e from the shear-center axis, Fig. 2b, can be treated in the same way, using the general solution represented by Eq. (4). In this case, the recurrence formula, analogous to Eq. (7a), becomes

$$[\xi(k\ell_n)]\phi''_n + [\eta(k\ell_n) + \eta(k\ell_{n+1})]\phi''_{n+1} + [\xi(k\ell_{n+1})]\phi''_{n+2} = [\zeta(k\ell_n)](qe)_n + [\zeta(k\ell_{n+1})](qe)_{n+1} \tag{7b}$$

where $\xi(k\ell)$ and $\eta(k\ell)$ are the same functions already introduced in Eqs. (8a) and the new function $\zeta(k\ell)$ is

$$\zeta(k\ell) = \frac{k\ell}{2} - \tanh\frac{k\ell}{2} \ . \tag{8b}$$

Also, for this case, the torque T_n just to the right of the support n is

$$T_n = \frac{C_1}{\ell_n}\left[\phi''_n - \phi''_{n+1}\right] + \frac{(qe)_n\ell_n}{2} \ , \tag{6b}$$

analogous to Eq. (6a). Equations (6b) and (7b) are sufficient to handle the case of a continuous beam under the action of uniformly distributed load.

Tf there are several concentrated loads in any span, or both concentrated loads and uniformly distributed load, it is only necessary to superimpose the appropriate right-hand members of Eqs. (7a) and (7b) and likewise the load terms in Eqs. (6a) & (6b).

To facilitate the use of the recurrence formula (7a) or (7b), the functions ξ, η, ζ, and ψ, defined by Eqs. (8a) and (8b), are recorded in Table I for a large range of values of $k\ell$.

Experimental Verification

As an experimental check on the foregoing theory, a simple test was made on a two-span beam as shown in Fig. 4. In this test, an eccentric transverse load P_1 was applied to a small pulley at the middle of span 1 and the corresponding angle of rotation ϕ was measured at the middle of span 2 by means of a reflected light-beam. The speciman used for this test was an aluminum alloy beam seventy inches long and having the balanced Z-section shown in Fig. 5. Free warping conditions at the supports were attained by using roller-type bearings oriented so as to prevent both rotation and lateral displacement of the supported cross-section in its plane but allowing complete freedom for longitudinal strain. For a load P_1 = 10 lb. applied with eccentricity e = 2.603 in. in span 1, the measured value of ϕ in span 2 was -0.00771 radians as compared with a calculated value of -0.00779 radians.

TABLE I

$k\ell$	ξ	η	ζ	ψ $a/\ell = 1/4$	ψ $a/\ell = 1/2$	ψ $a/\ell = 3/4$
0.00	0.0000	0.0000	0.0000	0.0000	0.0000	0.0000
0.10	0.0166	0.0333	0.0000	0.0004	0.0006	0.0005
0.20	0.0332	0.0665	0.0003	0.0016	0.0029	0.0022
0.30	0.0494	0.0994	0.0011	0.0035	0.0056	0.0049
0.40	0.0654	0.1319	0.0026	0.0061	0.0098	0.0086
0.50	0.0810	0.1640	0.0051	0.0095	0.0152	0.0134
0.60	0.0960	0.1953	0.0087	0.0135	0.0217	0.0191
0.70	0.1103	0.2260	0.0136	0.0181	0.0291	0.0257
0.80	0.1240	0.2559	0.0200	0.0233	0.0375	0.0331
0.90	0.1369	0.2850	0.0281	0.0290	0.0467	0.0414
1.00	0.1491	0.3130	0.0379	0.0350	0.0566	0.0503
1.10	0.1604	0.3401	0.0495	0.0415	0.0671	0.0598
1.20	0.1708	0.3662	0.0630	0.0483	0.0782	0.0699
1.30	0.1804	0.3913	0.0783	0.0553	0.0898	0.0805
1.40	0.1892	0.4151	0.0956	0.0629	0.1016	0.0916
1.50	0.1971	0.4381	0.1148	0.0697	0.1138	0.1029
1.60	0.2040	0.4600	0.1360	0.0771	0.1262	0.1146
1.70	0.2102	0.4809	0.1589	0.0845	0.1386	0.1265
1.80	0.2157	0.5006	0.1837	0.0918	0.1511	0.1385
1.90	0.2203	0.5195	0.2102	0.0991	0.1636	0.1507
2.00	0.2243	0.5373	0.2384	0.1063	0.1760	0.1629
2.10	0.2276	0.5542	0.2682	0.1134	0.1882	0.1752
2.20	0.2301	0.5704	0.2995	0.1203	0.2003	0.1874
2.30	0.2322	0.5855	0.3322	0.1270	0.2122	0.1996
2.40	0.2338	0.5999	0.3663	0.1335	0.2239	0.2118
2.50	0.2347	0.6136	0.4017	0.1398	0.2352	0.2238
2.60	0.2352	0.6265	0.4383	0.1459	0.2463	0.2357
2.70	0.2354	0.6387	0.4759	0.1518	0.2571	0.2474
2.80	0.2350	0.6503	0.5146	0.1574	0.2675	0.2590
2.90	0.2344	0.6613	0.5543	0.1628	0.2777	0.2705
3.00	0.2335	0.6717	0.5948	0.1679	0.2875	0.2817
3.10	0.2323	0.6815	0.6362	0.1728	0.2969	0.2928
3.20	0.2310	0.6908	0.6783	0.1775	0.3060	0.3036
3.30	0.2291	0.6997	0.7211	0.1819	0.3148	0.3143
3.40	0.2273	0.7081	0.7646	0.1861	0.3232	0.3247
3.50	0.2253	0.7161	0.8086	0.1901	0.3313	0.3349
3.60	0.2231	0.7237	0.8532	0.1939	0.3391	0.3450
3.70	0.2208	0.7309	0.8982	0.1974	0.3466	0.3548
3.80	0.2184	0.7378	0.9438	0.2008	0.3537	0.3644
3.90	0.2159	0.7444	0.9897	0.2040	0.3605	0.3737
4.00	0.2134	0.7507	1.0360	0.2069	0.3671	0.3829
4.10	0.2107	0.7566	1.0826	0.2097	0.3734	0.3919
4.20	0.2081	0.7623	1.1295	0.2124	0.3794	0.4006
4.30	0.2055	0.7678	1.1768	0.2149	0.3851	0.4092
4.40	0.2027	0.7730	1.2243	0.2172	0.3905	0.4175
4.50	0.2000	0.7780	1.2720	0.2194	0.3958	0.4257
4.60	0.1973	0.7828	1.3199	0.2214	0.4007	0.4337
4.70	0.1946	0.7874	1.3680	0.2234	0.4055	0.4414
4.80	0.1918	0.7918	1.4163	0.2252	0.4100	0.4490
4.90	0.1892	0.7960	1.4648	0.2268	0.4143	0.4564
5.00	0.1865	0.8001	1.5134	0.2284	0.4185	0.4636

TABLE I - (Continued)

$k\ell$	ξ	η	ζ	ψ $a/\ell = 1/4$	ψ $a/\ell = 1/2$	ψ $a/\ell = 3/4$
5.10	0.1839	0.8039	1.5621	0.2299	0.4224	0.4707
5.20	0.1813	0.8077	1.6110	0.2313	0.4261	0.4776
5.30	0.1787	0.8113	1.6599	0.2325	0.4297	0.4843
5.40	0.1762	0.8148	1.7090	0.2337	0.4331	0.4908
5.50	0.1736	0.8182	1.7581	0.2349	0.4363	0.4972
5.60	0.1712	0.8214	1.8074	0.2359	0.4394	0.5035
5.70	0.1687	0.8246	1.8567	0.2369	0.4423	0.5095
5.80	0.1663	0.8276	1.9060	0.2378	0.4451	0.5155
5.90	0.1640	0.8305	1.9555	0.2387	0.4478	0.5213
6.00	0.1617	0.8333	2.0049	0.2394	0.4503	0.5269
6.10	0.1594	0.8361	2.0545	0.2402	0.4527	0.5324
6.20	0.1572	0.8387	2.1040	0.2409	0.4550	0.5378
6.30	0.1550	0.8413	2.1537	0.2415	0.4572	0.5430
6.40	0.1530	0.8437	2.2033	0.2421	0.4593	0.5481
6.50	0.1508	0.8462	2.2530	0.2427	0.4613	0.5531
6.60	0.1488	0.8485	2.3027	0.2432	0.4632	0.5580
6.70	0.1468	0.8507	2.3524	0.2437	0.4650	0.5627
6.80	0.1449	0.8529	2.4022	0.2441	0.4667	0.5673
6.90	0.1429	0.8551	2.4520	0.2445	0.4683	0.5718
7.00	0.1411	0.8571	2.5018	0.2449	0.4698	0.5762
7.10	0.1391	0.8592	2.5516	0.2453	0.4713	0.5805
7.20	0.1374	0.8611	2.6015	0.2456	0.4727	0.5847
7.30	0.1356	0.8630	2.6513	0.2459	0.4740	0.5888
7.40	0.1339	0.8649	2.7012	0.2462	0.4753	0.5928
7.50	0.1322	0.8667	2.7511	0.2465	0.4765	0.5966
7.60	0.1306	0.8684	2.8010	0.2467	0.4776	0.6004
7.70	0.1290	0.8701	2.8509	0.2470	0.4787	0.6041
7.80	0.1274	0.8718	2.9008	0.2472	0.4798	0.6077
7.90	0.1259	0.8734	2.9507	0.2474	0.4808	0.6112
8.00	0.1243	0.8750	3.0007	0.2476	0.4817	0.6147
8.10	0.1229	0.8765	3.0506	0.2477	0.4826	0.6180
8.20	0.1215	0.8780	3.1005	0.2479	0.4834	0.6213
8.30	0.1200	0.8795	3.1505	0.2480	0.4842	0.6244
8.40	0.1186	0.8810	3.2004	0.2482	0.4850	0.6275
8.50	0.1172	0.8824	3.2504	0.2483	0.4857	0.6306
8.60	0.1159	0.8837	3.3004	0.2484	0.4864	0.6335
8.70	0.1146	0.8851	3.3503	0.2485	0.4871	0.6364
8.80	0.1133	0.8864	3.4003	0.2486	0.4877	0.6392
8.90	0.1121	0.8876	3.4503	0.2487	0.4883	0.6419
9.00	0.1109	0.8889	3.5002	0.2488	0.4889	0.6446
9.10	0.1097	0.8901	3.5502	0.2489	0.4894	0.6472
9.20	0.1085	0.8913	3.6002	0.2490	0.4899	0.6497
9.30	0.1073	0.8925	3.6502	0.2491	0.4904	0.6522
9.40	0.1062	0.8936	3.7002	0.2491	0.4909	0.6546
9.50	0.1052	0.8947	3.7501	0.2492	0.4913	0.6570
9.60	0.1041	0.8958	3.8001	0.2493	0.4918	0.6593
9.70	0.1030	0.8969	3.8501	0.2493	0.4922	0.6615
9.80	0.1019	0.8980	3.9001	0.2494	0.4926	0.6637
9.90	0.1009	0.8990	3.9501	0.2494	0.4929	0.6658
10.00	0.0999	0.9000	4.0001	0.2495	0.4933	0.6679

Numerical Calculations

The calculated value of ϕ is found in the following manner:

Aluminum alloy, $E = 10.5(10)^6$ psi, $G = 4.0(10)^6$ psi.
Length m of center-line of cross-section (see Fig. 5):

$$m = 1.319 + 0.2595 \times 2 + 0.919 \times 2 = 3.676 \text{ in.}$$

Torsional rigidity constant C:

$$C = \frac{1}{3}mt^3G = \frac{1}{3}(3.676)(0.081)^3 \times 4.0(10)^6 = 2605 \text{ lb.-in}^2.$$

Warping rigidity constant C_1:

$$C_1 = \frac{Etb^2}{12m}\left[4d^3(d+4b+2h) + 12hd^2(b+h) + 2h^2d(2b+3h) + h^2b(b+2h)\right].$$

$$C_1 = 16284 \quad [0.4594 + 2.385 + 5.232 + 5.687] = 224100 \text{ lb.-in}^4.$$

With C and C_1 determined, $k = \sqrt{C/C_1} = \sqrt{0.01162} = 0.1078$ in.$^{-1}$, and with $\ell_1 = \ell_2 = 35$ in., $k\ell_1 = k\ell_2 = 3.773$.

For $k\ell = 3.773$ and $a/\ell = 0.50$, Table I gives

$$\xi = 0.2191, \quad \eta = 0.7357, \quad \psi = 0.3516$$

Then with $\phi_1'' = \phi_3'' = 0$, Eq. (7a) becomes

$$0 + [0.7357 + 0.7357]\phi_2'' + 0 = 0.3516\left(\frac{0.1078}{2605}\right)(Pe)_1,$$

from which $\phi_2'' = 0.00000989(Pe)_1$.

Equation (6a) applied to span 2 now gives

$$T_2 = [0.00000989 - 0]\frac{224100}{35}(Pe)_1 = 0.0633(Pe)_1.$$

Elimination of ϕ_n' between the first and second of Eqs. (5), after replacing T_n by its value from Eq. (6a), gives

$$\phi_{n+1}' = \frac{\phi_n''}{k}\left[\xi(k\ell_n)\right] + \frac{\phi_{n+1}''}{k}\left[\eta(k\ell_n)\right] - \frac{(Pe)_n}{0}\left[\psi\left(\frac{a_n}{\ell_n}, k\ell_n\right)\right].$$

Applied to the two-span problem in hand, this becomes

$$\phi_2' = \frac{\phi_2''}{k}\left[\eta(k\ell_1)\right] - \frac{(Pe)_1}{0}\left[\psi\left(\frac{a_1}{\ell_1}, k\ell_1\right)\right].$$

Substitution of the value of ϕ_2'' already found above, together with η and ψ, gives

$$\phi_2' = \frac{9.89(Pe)_1}{0.1078(10)^6}(0.7357) - \frac{(Pe)_1}{2605}(0.3516) = -0.0000675(Pe)_1.$$

Finally, the angle of twist at the mid-point of span 2 is obtained from Eq. (2) which, for $z = \ell/2$, becomes

$$\phi = 0 + \frac{\phi_2'}{k} \sinh \frac{k\ell_2}{2} + \frac{\phi_2''}{k^2}\left(\cosh \frac{k\ell_2}{2} - 1\right) - \frac{T_2}{k^2}\left(\sinh \frac{k\ell_2}{2} - \frac{k\ell_2}{2}\right).$$

With the values of ϕ_2', ϕ_2'', and T_2, already found, this gives

$$\phi = (-0.002015 + 0.002016 - 0.0003003)(Pe)_1 = -0.0002993(Pe)_1.$$

Finally, for $P_1 = 10$ lb. and $e = 2.603$ in.,

$$\phi = -0.0002993 \times 26.03 = -0.00779 \text{ radians.}$$

BIBLIOGRAPHY

1. Timoshenko, S. P., "Theory of Bending, Torsion and Buckling of Thin-Walled Members of Open Cross Section." Journal of the Franklin Institute, Vol. 239; No. 3, March; No. 4, April; No. 5, May; 1945.
2. Goodier, J. N., "The Buckling of Compressed Bars by Torsion and Flexure." Bulletin No. 27, December, 1941, Cornell University Engineering Experiment Station, Ithaca, N. Y.
3. Engel, H. L., "Experimental Investigation of Elastic Torsion in the Presence of Initial Axial Stress." Technical Report No. 6 (Under direction of J. N. Goodier), January 31, 1950, Division of Engineering Mechanics, Stanford University, Stanford, California.
4. Wagner, H. and Pretschner, W., "Torsion and Buckling of Open Sections." Luftfahrtforschung, Vol. XI, No. 6, December 5, 1934, Verlag von R. Oldenbourg, Munchen und Berlin (NACA, T.M., No. 784).
5. Wagner, H., "Torsion and Buckling of Open Sections." Technische Hochschule, Danzig, (From 25th Anniversary Number, 1904-1929), (NACA, T.M., No. 807).
6. Kappus, Robert, "Twisting Failure of Centrally Loaded Open-Section Columns in the Elastic Range." Luftfahrtforschung, Vol. 14, No. 9, September 20, 1937, Verlag von R. Oldenbourg, Munchen und Berlin (NACA, T.M., No. 851).
7. Goldberg, John E., "Torsion of I-type and H-type Beams." American Society of Civil Engineers Transactions, Vol. 118, 1953.

Journal of the

ENGINEERING MECHANICS DIVISION

Proceedings of the American Society of Civil Engineers

CONTENTS

DISCUSSION

Note: Paper 2008 is part of the copyrighted Journal of the Engineering Mechanics Division, Proceedings of the American Society of Civil Engineers, Vol. 85, EM 2, April, 1959.

THE LATERAL RIGIDITY OF SUSPENSION BRIDGES[a]

Closure by I. K. Silverman

I. K. SILVERMAN,[1] A. M. ASCE.—The writer is indebted to Prof. Selberg for his comments. Prof. Selberg questions the validity of Eq. (7). The following assumptions were made in the development of (7):

(a) The increase in the H component of cable stress due to inertial forces can be neglected. This assumption has led to satisfactory results in the vertical analogue of the problem.
(b) The bending moment in the suspended span, as the result of neglecting inertial contribution to the H component, is given by Hu so that

$$M = -EI\nu'' = -HU$$

Eq. (7) then follows from (1) when the D'Alembert force is used as the lateral loading (In Eq. (1) the term $\frac{p\nu''}{h}$ should read $\frac{p\nu''}{H}$).

When H is of such magnitude, as for the extreme case of zero sag, so that u may be assumed to be zero, Eq. (7) becomes that of a simply supported span vibrating in a medium furnishing supporting forces proportional to the deflection ν. Another extreme case occurs when the stiffness of the suspended span is zero, i.e. EI = 0. Eq. (7) reduces in that case to that for a simple pendulum when the spring constant is $\frac{p}{h}$.

a. Proc. Paper 1292, July, 1957, by I. K. Silverman.
1. Engr., Bureau of Reclamation, U. S. Dept. of the Interior, Denver, Colo.

ON INELASTIC BUCKLING IN STEEL[a]

Discussion by P. P. Bijlaard

P. P. BIJLAARD,[1] M. ASCE.—Messrs. Haaijer and Thürlimann, in their dealing with buckling of structural steel plates in the horizontal part of the stress-strain diagram, say on page 1581-12 that, from the mathematical theory of plasticity, the stress-strain relations should be of the incremental type and that only the stress-strain law used by Handelman and Prager satisfies this condition, so that all other theories (including that of the discusser) can be discarded. They refer to tests on combined compression and torsion on tubes of mild steel in the horizontal part of the stress-strain diagram that confirm the stress-strain laws of simple flow theory. They then proceed to derive formulas which apply to this special case, for which they mainly refer to a preceding paper.(1)

It is the purpose of the present discussion to show that the authors' theoretical results, although not stated that way, are actually based on the discusser's theory, as published in various papers in the past twenty years.(2,3,4,5,6,7,8) In the first place the discusser's theory includes both deformation and incremental theory, as pointed out in all his papers and has been stated elsewhere.(9) The stress-strain relations for simple flow theory as derived by Handelman and Prager (1948), follow directly from the discussor's theory, published in 1938, by assuming $e = \epsilon_p/\epsilon_e = 0$, where ϵ_p and ϵ_e are the equivalent plastic and elastic strains at incipient buckling and for the special case of uniaxial compression discussed by them ($\beta = 0$) (reference 2, p. 480 and ref. 3, p. 733), or, with other notations, for $E_s/E = 1$, where E_s is the secant modulus at incipient buckling (ref. 6, 7 and 8). In papers published before World War II, since he concluded from earlier tests on aluminum alloy angles by Kollbrunner that the assumption $e = 0$ (incremental theory) would lead to much too high theoretical buckling stresses, the discussor assumed deformation theory, which he showed to give a lower bound for the buckling stress, admitting the possibility that for structural steel this might slightly underestimate the buckling stress (ref. 3, pp. 733, 734). For buckling below the yield point, the only case that had to be considered for structural steel, ϵ_p is small, and hence e is small, so that incremental or flow theory gives only slightly higher results. Also, using deformation theory, the resulting buckling stresses were already much higher than according to Chwalla's theory (using the same plastic reduction factor for plates as for columns) which at that time in Europe was assumed to be right. He also showed that experiments on steel plates by Chase, buckling at the yield point, were in good agreement with incremental theory (ref. 3, p. 740).

---

a. Proc. Paper 1581, April, 1958, by Geerhard Haaijer and Bruno Thürlimann.

1. Prof. of Mechanics, Cornell Univ., Ithaca, N. Y.

In papers published after World War II (ref. 5) the discusser concluded from new tests by Kolbrunner on aluminum alloy plates,[10] that, using deformation theory, his theoretical results were in excellent agreement with these experiments and further developed his theory for aircraft structures (ref. 6 and numerous later papers in the Journal of the Aeronautical Sciences), showing also excellent agreement with tests by the NACA and others.[8] His theory is now generally used in aircraft design,[11,12] sometimes with Stowell's simplification (Poisson's ratio in the elastic range is 0.5).[9]

That in certain cases deformation theory would lead to impossible results was already shown by the discussor on page 734 of reference 3. However, this does not mean that in the special case of buckling, where the ratio between the stress components changes very smoothly, the actual behavior cannot be similar to what would follow from deformation theory, although it may be different in other cases than buckling, that is, for non-linear behavior. In references 6 and 8 the writer showed how this behavior, which is in accordance with buckling tests on aluminum alloys, can be explained. It does not conflict with the theory of plasticity.[13] It places the general behavior between that according to deformation and simple flow (incremental) theory, as it actually is.[6,7] In this connection it may be noted that, although in this country flow theory is used for problems other than buckling, in Russia deformation theory is used. Batdorf and Budiansky's slip theory, which is theoretically sound, but was not completely confirmed by non-buckling tests on compressed and twisted tubes, for the case of buckling also reduces to deformation theory.[14] The actual behavior of a polycrystalline metal under all kinds of stress variations could only be predicted by a theory based on the interaction of its dislocations, flaws, etc., which does not exist, but as explained in references 6 and 8 and others, for the special case of buckling of materials like aluminum, magnesium, titanium alloys and high strength steels, and in an approximate way, for mild steel below the yield point, the behavior is similar to that according to deformation theory (but may be generally incremental). As was shown in reference 15 for aluminum the assumption of eccentricities, as suggested by Onat and Drucker,[16] does not lead to an agreement between simple flow theory and buckling tests.

However, as already observed on page 55 of reference 17, it is completely understandable from the discusser's theory that in the horizontal part of the stress-strain diagram of mild steel, which is considered by the authors, the behavior is close to simple flow (incremental) theory. His explanation of the behavior of aluminum alloys[6,8] is based on the fact that, due to unavoidable small eccentricities or due to Shanley's principle of simultaneous action, the buckling stress increases during buckling. In the horizontal part of the stress-strain diagram this increase is impossible, so that the same case occurs as in a tube which, after subjecting it to compression, is twisted while keeping the compressive stress constant. In this case, as follows from the authors' tests and also from earlier tests by Hohenemser and Prager,[18] to which the discusser referred in reference 2 and 3 (pp. 480 and 733, respectively), the material behaves indeed in accordance with incremental theory. Hence, here the discusser's theory applies, with $e = 0$ or $E_s/E = 1$.

The authors assume that in this horizontal part of the stress-strain diagram, at buckling the entire cross section behaves in a plastic way, based on a proof given in reference 1. The discusser already has proved that in a similar way in references 2 and 4, pages 476 and 52, respectively, mentioned in reference 9 of their paper. It may be noted that it cannot be derived from

Shanley's principle, since in the present case the direct stress does not increase during buckling.

On page 2 and in their summary the authors say that 'til now it was assumed that at the yield stress a plate has no rigidity against buckling. As pointed out in reference 2 the discusser actually developed his theory on the plastic buckling of plates with the purpose of showing that at the yield stress a plate has still a considerable rigidity against buckling (as also noted in reference 6, to prove his theory on the deformations of the earth's crust). He emphasized the same point in later papers and in a report to the Column Research Council,[19] so that this may be assumed to be known since a long time.

For the basic formulas in the authors' paper, for which they refer to reference 1, they could more appropriately have referred to the discusser's papers. In the discusser's notation their constants are

$$D_x = EA \; ; \; D_y = ED \; ; \; H = E(B+2F) ; \; D_{xy} = D_{yx} = EB ; \; G_t = EF \qquad (1)$$

The values A, B, D and F, where in the present case e = 0 or E_s/E is one, can, for example, be obtained from reference 6 as functions of E, E_t ρ_1, ρ_2 and Poisson's ratio ν in the elastic range, where in the authors' notations, $\rho_1 = \sigma_x$ and $\rho_2 = \sigma_y$. For example, their value $G_t = d\tau/d\gamma = 2400$ ksi was obtained from Eqs. (6.4) and (6.5) of reference 1, where, from Eq. (4.16) of reference 1,

$$F = \frac{3}{4J_2}\left(\frac{1}{E_t} - \frac{1}{E}\right)$$

Hence, from these Eqs. (6.4) and (6.5)

$$\frac{d\gamma}{d\tau} = \frac{2(1+\nu)}{E} + 4F\tau^2 = \frac{2(1+\nu)}{E} + \frac{3}{J_2}\,\frac{E-E_t}{EE_t}\,\tau^2 \qquad (2)$$

This formula follows directly from Eqs. (10) and (18) of the discusser's paper in reference 5, which is the authors' reference 9, which equations also occur in an earlier report of the discusser to the sixth International Congress of Applied Mechanics, Paris, 1946. They give

$$\frac{\partial\gamma}{\partial\tau} = \frac{\partial\gamma_e}{\partial\tau} + \frac{\partial\gamma_p}{\partial\tau} = \frac{1}{G} + \frac{1}{G_p} + \frac{3\tau^2}{\sigma_q^2 G_p}\left(\frac{E_p}{\tan\varphi} - 1\right)$$

where in the authors' notations (see p. 536 of ref. 6)

$$E_p/G_p = 3 \; ; \; \sigma_q^2 = \tfrac{3}{2}S_1^2 = 3J_2 \; ; \; \tan\varphi = \frac{EE_t}{E-E_t}$$

In the present case, e = E/Ep = 0, or Ep = G_p = infinite, so that one gets

$$\frac{\partial\gamma}{\partial\tau} = \frac{1}{G} + \frac{9\tau^2}{3J_2}\,\frac{E-E_t}{EE_t} = \frac{2(1+\nu)}{E} + \frac{3}{J_2}\,\frac{E-E_t}{EE_t}\,\tau^2 \qquad (3)$$

which is identical to Eq. (2). In the same way Eqs. (6.6) and (6.7) of reference 1, from which the authors' values D_x, D_y and D_{xy} are computed, are identical to the discusser's formulas[19] in reference 5.

As a last point the discusser may refer to the authors' Eqs. (10) to (17) which, instead of deriving them in reference 1, without reference to the discusser's results, could have been obtained directly from Table 5 of reference

6, where the plastic reduction factors η are given, where the well known elastic buckling stresses σ_e have to be multiplied with to obtain the plastic buckling stresses σ_{cr}. This would also have avoided errors as occur in their case.(2)

First their cases (1), (3) and (4) will be considered.

(1) Loaded edges x = 0 and x = ℓ hinged, unloaded edge y = 0 hinged and unloaded edge y = b free. Using Eqs. (1), with $\nu = 0.3$, from Table 5 of reference 6

$$\sigma_{cr} = \eta\sigma_e = 2.6\,F G_j \left(\frac{t}{b}\right)^2 = 2.6\,F \frac{E}{2.6}\left(\frac{t}{b}\right)^2 = G_t \left(\frac{t}{b}\right)^2$$

in accordance with the authors' Eq. (11). Their more general Eq. (10) is identical to Eq. (34) of reference 5.

(2) Loaded edges x = 0 and x = ℓ hinged, unloaded edges y = $\pm$ d/2 hinged. From Table 5 of reference 6

$$\sigma_{cr} = \eta\sigma_e = 0.455\left(\sqrt{AD} + B + 2F\right)\frac{4\pi^2 E}{12(1-\nu^2)}\left(\frac{t}{d}\right)^2$$
$$= \frac{\pi^2}{12}\left(\frac{t}{d}\right)^2\left(2\sqrt{D_x D_y} + 2D_{xy} + 4G_t\right)$$

in accordance with the authors' Eq. (15), since $D_{yx} = D_{xy}$.

(3) Same as case 2, but unloaded edges y = $\pm$ d/2 fixed.

$$\sigma_{cr} = \eta\sigma_e = \left[0.598\sqrt{AD} + 0.312\left(B + 2F\right)\right]\frac{6.99\pi^2 E}{12(1-\nu^2)}\left(\frac{t}{d}\right)^2$$
$$= \frac{\pi^2}{12}\left(\frac{t}{d}\right)^2\left[4.60\sqrt{D_x D_y} + 2.40\left(D_{xy} + 2G_t\right)\right]$$

which is practically in accordance with the authors' Eq. (17).

(4) Same as case 1, but unloaded edge y = 0 fixed. From Table 5 of reference 6

$$\sigma_{cr} = \eta\sigma_e = 0.473\left(\sqrt{AD} + 2.97F - 0.405B\right)\frac{1.28\pi^2 E}{12(1-\nu^2)}\left(\frac{t}{d}\right)^2$$
$$= \left(\frac{t}{d}\right)^2\left(0.546\sqrt{D_x D_y} - 0.221\,D_{xy} + 1.62\,G_t\right) \qquad (4)$$

In contrast, the authors obtain in their Eq. (13)

$$\sigma_{cr} = \left(\frac{t}{d}\right)^2\left(0.769\sqrt{D_x D_y} - 0.54\,D_{xy} + 1.712\,G_t\right) \qquad (5)$$

which is similar to Eq. (3.15) of reference 1. It is obvious that the authors' formula (13) must be in error, since in the elastic range it does not reduce to the elastic buckling stress

$$\sigma_{cr} = 1.28\frac{\pi^2 N}{d^2 t} = 1.16\,E\left(\frac{t}{d}\right)^2 \qquad (6)$$

Since in the elastic range $D_x = D_y = E/(1-\nu^2)$, $D_{xy} = E\nu/(1-\nu^2)$ and $G_t = G = E/(2+2\nu)$, with $\nu = 0.3$, the authors' Eq. (13) yields $\sigma_{cr} = 1.325\,E\left(\frac{t}{d}\right)^2$.

Hence one should better use the present Eq. (4).

Since the authors' method of computation requires the assumption of unknown eccentricities for determining the buckling stress or critical strain, it is necessarily very arbitrary. For example, their value $\mathcal{G}_t$ = 2400 ksi is based on Fig. 10 of reference 1, from which $\mathcal{G}_t$ could have been chosen just as well as 1500 or 3000 ksi. Their method is therefore not capable of predicting the critical strains but has to be based on tests. The authors should therefore be complimented on their careful and important experiments, on which their selection of the values for $\mathcal{G}_t$, D_x, D_y and D_{xy} is mainly based.

REFERENCES

1. Haaijer, G., "Plate Buckling in the Strain-Hardening Range", Proceedings of the ASCE, Journal of the Engineering Mechanics Division, April 1957.
2. Bijlaard, P. P., "A Theory of Plastic Buckling with its Application to Geophysics," Proceedings Royal Netherlands Acad. of Sciences, Amsterdam, Vol. 41, No. 5, pp. 468-480, May 1938.
3. Bijlaard, P. P., "A Theory of Plastic Stability and its Application to Thin Plates of Structural Steel," Proceedings Royal Netherlands Acad. of Sciences, Amsterdam, Vol. 41, No. 7, pp. 731-743, September 1938.
4. Bijlaard, P. P., "Theory of the Plastic Stability of Thin Plates," Publ. Internat. Assoc. of Bridge and Struct. Engineering, Zürich, Vol. 6, pp. 45-69, 1940-41.
5. Bijlaard, P. P., "Some Contributions to the Theory of Elastic and Plastic Stability," Publ. Internat. Assoc. of Bridge and Struct. Engineering, Zürich, Vol. 8, pp. 17-80, 1947.
6. Bijlaard, P. P., "Theory and Tests on the Plastic Stability of Plates and Shells," Journal of the Aeron. Sciences, Vol. 16, No. 9, pp. 529-541, 1949.
7. Bijlaard, P. P., "On the Plastic Buckling of Plates According to the Flow Theory," Journal of the Aero. Sciences, Vol. 17, No. 12, pp. 810-811, 1950.
8. Bijlaard, P. P., "Theory of Plastic Buckling of Plates and Application to Simply Supported Plates Subjected to Bending or Eccentric Compression in their Plane", Jour. of Applied Mechanics, Vol. 23, No. 1, pp. 27-34, 1956.
9. Gerard, G. and Becker, H., "Handbook of Structural Stability, Part I—Buckling of Flat Plates," NACA TN 3781, July 1957.
10. Kollbrunner, C. F., "Das Ausbeulen der auf einseitigen, gleichmässig verteilten Druck beanspruchten Platten im elastischen und plastischen Bereich," Mitt. a. d. Institut fur Baustatik a.d. E.T.H., Zürich, Switzerland, No. 17, 1946.
11. Krivetsky, A., "Plasticity Coefficients for the Plastic Buckling of Plates and Shells," Journal of the Aeronautical Sciences, Vol. 22, No. 6, pp. 432-435, 1955.
12. Sechler, E. E., "Inelastic Buckling—From the Designer's Viewpoint," Journal of the Aeronautical Sciences, Vol. 23, No. 5, pp. 500-506, 1956.

13. Drucker, D. C., "A Discussion of the Theories of Plasticity," Journal of the Aeronautical Sciences, Vol. 16, No. 9, pp. 567-568, 1949.

14. Batdorf, S. B., "Theories of Plastic Buckling," Journal of the Aeronautical Sciences, Vol. 16, No. 7, pp. 405-408, 1949.

15. Bijlaard, P. P. and Wiseman, H. A. B., "On Theories of Plasticity and the Plastic Stability of Cruciform Sections," Vol. 20, No. 11, pp. 787-788, 1953.

16. Onat, E. T. and Drucker, D. C., "Inelastic Instability and Incremental Theories of Plasticity," Journal of the Aeronautical Sciences, Vol. 20, No. 3, pp. 181-186, 1953.

17. Bijlaard, P. P., "Buckling of Columns, with Special Attention to Eccentricity, Plasticity and Local Buckling," Proceedings of the Seventh Technical Session of the Column Research Council, pp. 37-65, 1958.

18. Hohenemser, K. and Prager, W., "Beitrag nur Mechanik des bildsamen Verhaltens von Flusstahl," Zeitschrift f. angew. Math. u. Mechanik, Vol. 12, pp. 1-14, 1932.

19. Bijlaard, P. P., "Some Remarks on Chapter IX and Some Other Items in Bleich 'Buckling Strength of Metal Structures'," Report to Column Research Council, 1952.

INCREMENTAL COMPRESSION TEST FOR CEMENT RESEARCH[a]

Closure by A. Hrennikoff

A. HRENNIKOFF,[1] M. ASCE.—The writer is somewhat disappointed in the small extent of the response to his paper describing what he believes to be a new approach to the study of creep in cement. This makes him particularly grateful to the sole contributor to the subject, Mr. Keith Jones, for his thoughtful discussion of the paper.

Mr. Jones' particular interest lies in the creep of concrete. Although the writer's work so far involved no concrete but only cement and partly mortar, he feels that the creep of concrete originates primarily in cement, although the presence of aggregate modifies it in a significant manner.

Mr. Jones makes special reference to one of the results obtained from the incremental tests, namely the regularity of values of the coefficient of lateral deformation $\mu = \frac{\Delta\epsilon\,(\text{lateral})}{\Delta\epsilon\,(\text{longitudinal})}$. The values of μ during all stages when the load is changed are virtually constant and equal to about 0.2, both in the moist cylinders and in the dry ones of the same composition. On the other hand, the values of μ observed in the moist cylinders while the load is kept constant are different at different load levels, although they tend to remain constant at each particular level. While on the way up, the values of μ are close to zero on the lower steps of 10 and 15 kips, and they grow from step to step rising as high as 0.2 or even higher on the 35 kips step. On the way down the values of μ during creep are close to zero on the upper steps and increase to 0.10 - 0.12 on the levels 0 and 5 kips. This behaviour strongly suggests that creep is not the same kind of deformation, only developed gradually, as the one that is taking place while the load is being changed, but is something entirely different.

The regularity in the values of the μ stated here has been observed consistently in a great number of tests, but the exact magnitude of the lower values of μ is somewhat uncertain in view of the smallness of the deformations involved and the difficulty of obtaining the necessary sensitivity of the measuring apparatus. Thus the longitudinal deformation at 10 kips level in Fig. 9 is estimated at 23 micro-inches per unit. An error of little as one micro-inch per inch in reading the lateral deformation would change μ by a substantial quantity of 1/23 - 0.043. Errors of two or three times this amount may be expected in the lateral gauge used in spite of its refinements, such as invar metal for its segments and isoelastic springs for the sensitive elements. While during the load changes and on the constant load steps with great amount

---

a. Proc. Paper 1604, April, 1958, by A. Hrennikoff.

1. Prof., Dept. of Civ. Eng., Univ. of British Columbia, Vancouver, B. C., Canada.

of creep the inaccuracies in the computed mechanical properties, resulting from errors in strain measurement, are small, on the steps with small creep they are such as to make the computed values of μ unreliable.

Most of the tests including the ones involving the specimen C.58 (Fig. 9 and 10) show negative values of μ on the lowest horizontal step, on the way up, indicating a decrease rather than increase of the diameter of the specimen, in the course of contraction of its length under the action of creep. The writer attributed the negative reading of the lateral deformation to the errors of the gauge and assumed the corresponding true value of μ to be zero. There is however a possibility that the contraction of the diameter is a genuine phenomenon brought about in the following manner. As the load on the specimen is quickly increased its length is elastically decreased, and so is the volume, as the elastic value of $\mu = 0.2$ is less than the value 0.5 required for the constancy of the volume. The decrease in volume is accompanied by a decrease in void space, occupied largely by water, which is thus brought under compression, producing a bursting action on the cylinder. The cylinder is thus extended laterally not only by the elastic Poisson's ratio effect, but also by the tension created by the pressure of water occupying its voids. In the period of time when the load is kept constant the water, in an action similar to clay consolidation, drains from the voids where it is confined under compression, into the numerous air voids scattered throughout the cement mass. The disappearance of pressure from the water results on the one hand in an increase of the longitudinal stress in the cement skeleton, causing its longitudinal creep, and on the other hand it causes a contraction of cement in the lateral direction, occasioned by the disappearance from it of the lateral tension.

The effect of the bursting action of water described here on the longitudinal creep and on the lateral negative creep may be true, but its extent, as is believed by the writer, is very small. Instruments of extreme sensitivity and accuracy, greatly exceeding the ones used by the writer, are needed to prove the existence of negative lateral creep.

In his more recent studies the writer has discovered what appears to be the major cause of creep in moist cement. It is the slow deformation of the water film enveloping the elements of cement gel. The film is held to cement by a strong attraction, which transforms the water of the film into a viscous solid. The writer does not wish at this stage to go more extensively into this matter because it is a subject of another paper of his, now under review by ASCE.

The writer regrets to be unable to answer with certainty the question of the discusser with regard to the values of μ during creep in dry specimens. The values of longitudinal creep in these cylinders are very small, and of the lateral creep—even smaller. Thus the total longitudinal creep on all seven steps on the way up in the cylinder 6C32 (Fig. 14) amounts to only 120 microinches per inch with perhaps 30 units being the greatest value on any one step. An error of one or two units in the lateral strain would result in a totally misleading value of μ. It appears that creep in the dry cylinders is caused by minor internal breakages, accentuated by minute cracks formed in the course of drying. Apart from tendency for the somewhat greater amounts of creep at the higher levels compared to the lower ones, no other regularities with regard to creep in dry cylinders have been observed.

The writer expresses hope that in spite of the lack of discussers his method of experimental study of the mechanical properties of cement in

general and creep in particular will not pass unnoticed by the research workers in the field of cement and concrete.

CORRECTIONS.—Page 1604-12, 6th line of the third paragraph should be "anomaly", not "anamoly".

Same page, 9th line of third paragraph should be "on loading", rather than "and unloading".

Page 1724-4, corrections to the paper in July 1958 issue of the Journal, "Fig. 10" is left out from under the figure.

THE ELASTIC STABILITY OF THIN SPHERICAL SHELLS[a]

Discussion by Wen Liang Chen

WEN LIANG CHEN,[1] J. M. ASCE.—In the determination of critical pressure from the expression of total potential energy it was assumed in this paper that the parameter C is constant for a given shell in order to reduce the computational work. As pointed out by the author in his Sc.D. thesis,(1) on which this paper is based, experimental results of Kaplan and Fung(2) showed that for a given shell the mode of deflection changes during the loading process such that in actuality the parameter C is not constant for a given shell. The author reasoned that, since his investigation is concerned with the determination of buckling pressures, rather than deflection shapes, it is possible that an incorrect deflection equation may still yield a fairly good approximation of the critical load.

During the course of research for the writer's Sc.D. thesis(3) the critical pressure was determined from the expression of total potential energy used by von Willich in such a way that the assumption of constant C was avoided. The total potential energy was minimized with respect to both parameters w_o and C. Computation was carried out on the I.B.M. 704 computer in the M.I.T. Computation Center. Fig. 1 shows the comparison of the theoretical results. Curves 1 and 2 are results obtained by the method of minimizing the total potential energy with and without the assumption of constant C, respectively. The agreement between Curves 1 and 2 is fairly good for lambda equal to or less than 5 with a maximum discrepancy of 15%. However, the discrepancy increases rapidly to 41% as lambda increases from 5 to 6. Thus, the proximity of Curve 1 to the experimental points in the range $5 < \lambda < 8$ is accidental, since the elimination of one assumption in the computation gives results of Curve 2.

Also shown in Fig. 1 are the results of Archer,(4) given by Curve 3 which are obtained from perturbation solution of the governing non-linear differential equations, and the results of Weinitschke,(5) given by Curve 4 which are obtained from power series solution of the governing non-linear differential equations. The dotted portion of Curve 4 is a lower bound to the critical pressure given in Reference 5. It can be seen from Fig. 1 that for $\lambda < 5.5$ there is good agreement between the results obtained from the minimal principle by the writer and from either the power series solution or the perturbation solution of the non-linear differential equations. For $\lambda > 5.5$ Curve 2 rises very rapidly and is inaccurate probably because the assumed deflection with respect to which the total potential energy is minimized is not of sufficient generality.

---

a. Proc. Paper 1897, January, 1959, by Gideon P. R. von Willich.

1. Graduate Student, Massachusetts Inst. of Technology, Cambridge, Mass.

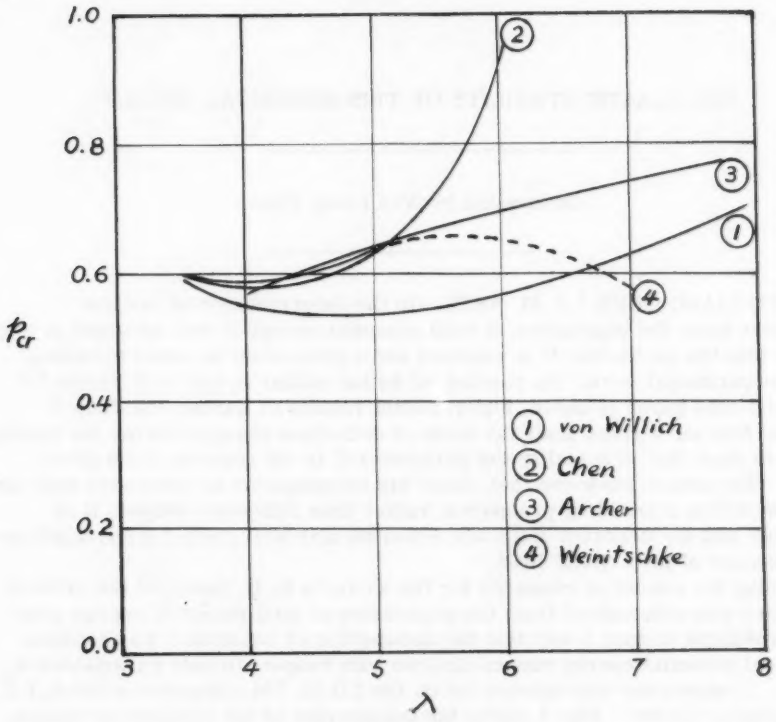

Figure 1

An investigation is reported in Reference 3 in which the effect of initial geometrical imperfection of the middle surface of shell on the buckling pressure is found to be quite significant and could account for the scatter of experimental results.

REFERENCES

1. Gideon P. R. von Willich. The Elastic Stability of Thin Spherical Shells. Sc.D. Thesis, Department of Civil and Sanitary Engineering, Massachusetts Institute of Technology, 1957.

2. A. Kaplan and Y. C. Fung. A Non-linear Theory of Bending and Buckling of Thin Elastic Shallow Spherical Shells. U. S. N.A.C.A. Technical Note 3212, 1954.

3. Wen Liang Chen. Effect of Geometrical Imperfection on the Elastic Buckling of Thin Shallow Spherical Shells. Sc.D. Thesis, Department of Civil and Sanitary Engineering, Massachusetts Institute of Technology, January 1959.

4. R. R. Archer. Stability Limits for a Clamped Spherical Shell Segment Under Uniform Pressure. Quarterly of Applied Mathematics, Vol. XV, No. 4 (1958).

5. H. J. Weinitschke. On the Non-linear Theory of Shallow Spherical Shells. Journal of the Society for Industrial and Applied Mathematics, Vol. 6, No. 3, pp. 209-232 (1958).

SIMPLIFICATION OF DIMENSIONAL ANALYSIS[a]

Discussion by Turgut Sarpkaya

TURGUT SARPKAYA,[1] A. M. ASCE.—Since its inception by Vaschy and later its emphatic presentation and popularization by Buckingham, dimensional analysis has enjoyed a particular esteem among engineers as well as mathematicians. There are, to be sure, rather comprehensive treatments of the subject some of which are concerned mainly with its philosophical aspects, some with its mathematical foundations, and some with its practical applications. However, any effort made toward a better determination of the limitations of dimensional analysis and toward the simplification of the formation of Pi-terms, such as made by the authors, is a welcome contribution.

The question has been raised as to the effectiveness of dimensional analysis. This writer believes that as a tool alone it is impressive rather than powerful. It should be made quite clear that no useful result could be deduced from dimensional analysis unless it is accompanied by experience, experiments, strong intuition, inspectional analysis, and by a close familiarity with the phenomenon. Since its application to a given problem depends very much on personal considerations, it is no better and no worse than the researcher's understanding of the particular phenomenon. It should also be made quite clear that even if the entire analysis is performed meticulously, the researcher should still expect unexpected deviations from the analysis at certain points or regions, (Constanzi-Eiffel paradox and some other hydrodynamical paradoxes.(1)) Furthermore, although one is closer to his goal after dimensional considerations, the final and best grouping of variables and the extent of the accomplishment attained still remains to be determined. Indeed, one is seldom sure until one has all the necessary experimental results whether certain Pi-term or terms are worth forming.

In a practical application, once the independent variables are determined and the repeating variables are judiciously selected, the application of the Pi-theorem itself is a purely mechanical process, no matter which one of the following methods is used: conventional determinant method, the method of special arrangement of the variables in the determinant form, and the method of selection of repeating variables to represent the dynamic, kinematic, and geometric variables.

A fourth method, devised by this writer(2) about six years ago for the formation of Pi-terms, is by means of vectors in a three dimensional logarithmic coordinate system, (four dimensional for heat transfer, electric potential or charge problems). Only the basic ideas will be presented here for practical applications. The demands of mathematical rigour may be found in the reference sited.

---

a. Proc. Paper 1898, January, 1959, by Charles C. Bowman and Vaughn E. Hansen.

1. Asst. Prof., Eng. Mechanics Dept., Univ. of Nebraska, Lincoln, Nebr.

An axis L^n, and an ordinate T^n, is taken as shown in Fig. 1. The scale on each axis is logarithmic, and the origin of the coordinate system is unity. Each point (n.L), or (n.T), distance from the origin represents L^n, and T^n, respectively. n is an ordinary real number and L, and T, are unit quantities. Then the following vectorial operations are self explanatory:

$$AB = L.T^2, \quad AC = L^3.T, \quad CA = L^{-3}.T^{-1}, \quad BC = L^2.T^{-1}, \quad CB = L^{-2}.T$$

$$AC/AB = L^2.T^{-1} = BC$$

The nature of the axes is such that to divide or to multiply one vector by another, an equivalent and parallel vector must be drawn. If a division is to be performed, the vector is drawn in the opposite direction; if multiplication, in the same direction. It is significant to note that in the new vector system the ratio of the lengths of parallel vectors is equal to the ratio of their exponents. It is extremely important also to note that each closed polygon in this coordinate system (two or three dimensional), reduces to unity as long as one is consistent with the direction of rotation, clockwise or counter-clockwise. Referring again to Fig. 1, it is seen that

$$AB.BC.CA = L.T^2 \cdot L^2.T^{-1} \cdot L^{-3}.T^{-1} = 1$$

One can now examine the system more generally where the operations are made in a three dimensional space in which each point is represented by (L^n, M^n, T^n), and each vector by ($L^n \cdot M^n \cdot T^n$). As will have become evident from the foregoing explanations, the properties of the two dimensional coordinate system hold true for the three dimensional case as well.

Having established the fundamental concepts of the coordinate system one can employ it in the formation of Pi-terms. If the meanings length, mass, and time are assigned to L, M, and T, respectively, then the vectors in Fig. 2, represent the dimensions of various physical quantities as follows: OA,

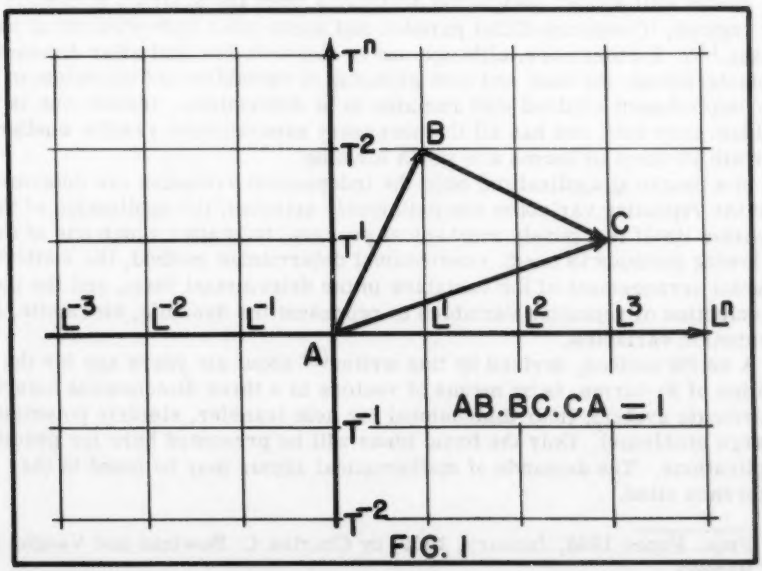

FIG. 1

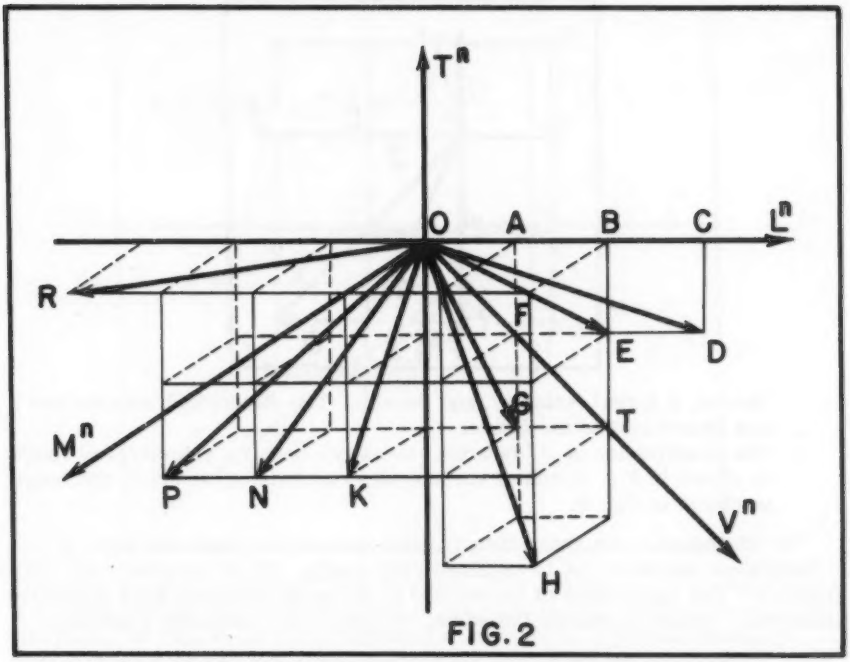

FIG. 2

length; OB, area; OC, volume; OD, discharge; OE, kinematic viscosity, circulation, or unit discharge; OF, velocity; OG, acceleration; OH, heat transferred per unit time; OK, surface tension; ON, pressure intensity, elastic modulus, or shear intensity; OP, specific weight; and OR, the mass density. Obviously, geometric quantities are on L^n, axis, kinematic quantities are in (L^n, T^n), plane, and dynamic quantities are in (L^n, T^n, M^n), space. Each vector in this system represents the dimensions of products which may or may not have a physical meaning. Every vector such as OF in Fig. 2, actually represents the n-th power of the dimension vector, ($OT = V^2$), and usually in the case of $n = 1$, has a physical meaning. As far as the selection of repeating variables is concerned, it is well known that the determinant of the exponents of repeating variables must not be equal to zero. It can be seen very easily that in the vectorial system this mathematical condition corresponds to the condition that the vectors representing the dimensions of repeating variables must not form a closed polygon. For example, the vectors corresponding to area, velocity, and mass density cannot form a closed polygon regardless of the value of their exponents.

To illustrate the method, the following examples are given:

1. The combination of V (velocity), D (length), and g (gravitational acceleration), is desired. In Fig. 3, these vectors are first drawn, and then a closed polygon is formed. From the small triangle, rotating in the clockwise direction, one obtains: $V.D^{-1/2}.g^{-1/2}$. Similarly, from the large triangle: $V^2.D^{-1}.g^{-1}$, is obtained.
2. The combination of ρ (density), V (velocity), and p (pressure), is shown in Fig. 4. In the same figure, one can also see the combination of F

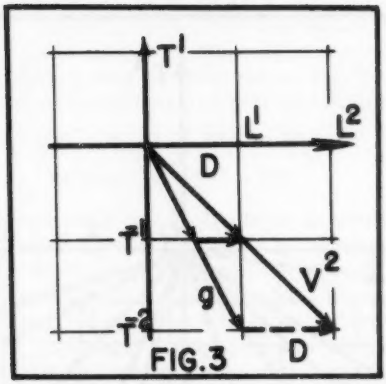

FIG. 3

(force), A (area), velocity, and density. The dimensionless numbers are shown next to the figure.

3. The combination of μ (dynamic viscosity), density, velocity, and length is shown in Fig. 5; and of surface tension, density, velocity, and length is shown in Fig. 6.

The examples given above clearly show that all the other classical dimensionless numbers can be obtained very easily. All is necessary is a little practice. The application of the method to the systems which have more than three basic units, is exactly the same. To prove the statement a problem

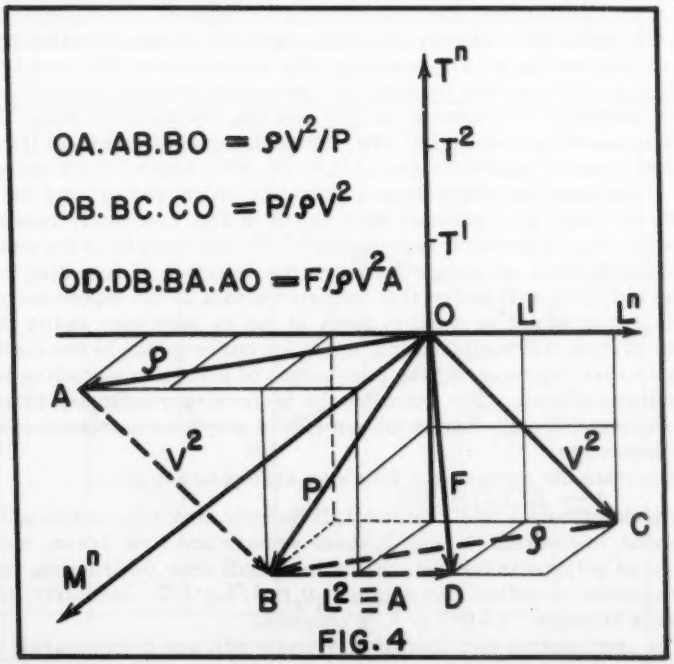

FIG. 4

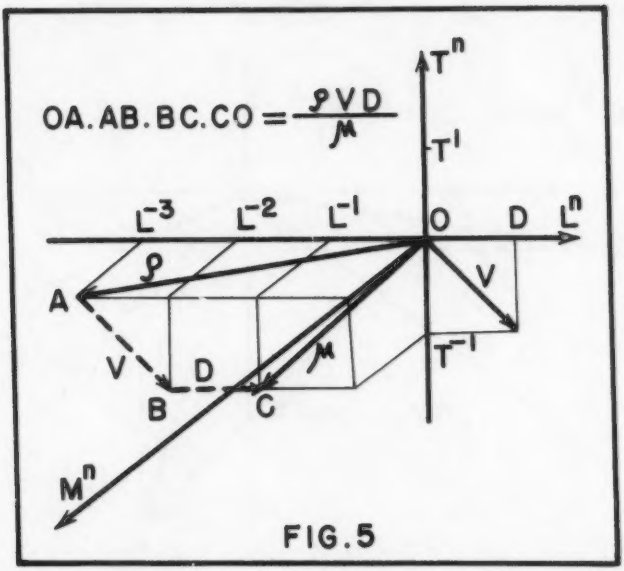

FIG.5

involving the transference of heat is given. The temperature is regarded as a quantity not yet reducible in terms of the fundamental units of mass, length, and time. In Fig. 7, the combination of ϵ (specific heat per unit mass), H (heat transferred per unit time), θ (absolute temperature), D (a characteristic length), and mass density is shown in detail.

In the examples given above, axes were taken as L^n, M^n, T^n, and θ^n. It is perfectly permissible to use L^n, F^n, T^n, and θ^n, which may be more helpful to the engineer who is accustomed to using force rather than mass. In

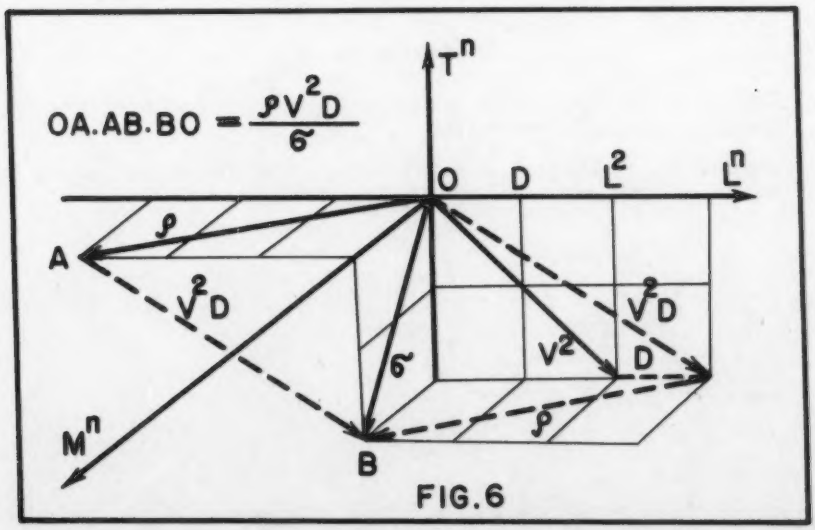

FIG.6

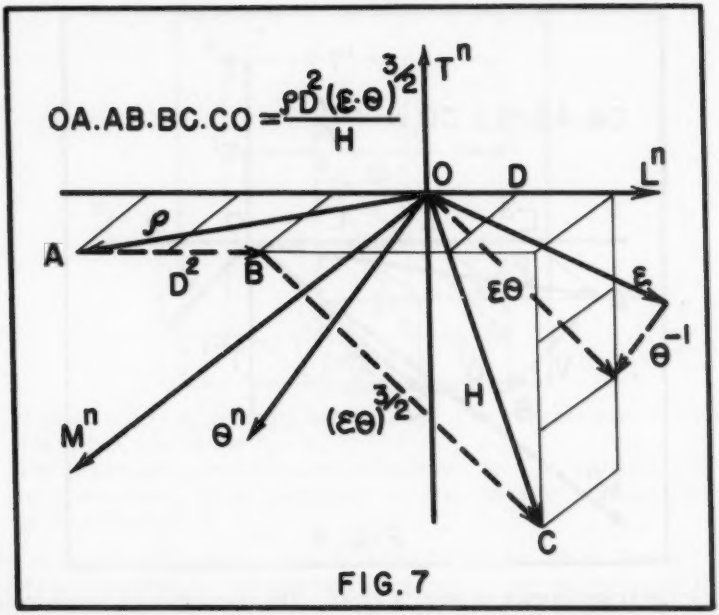

FIG. 7

electrical engineering problems the axes could be chosen either as L^n, M^n, T^n, and Q^n, or as L^n, M^n, T^n, and ϕ^n, in which Q, and ϕ, represent the electric charge and the electric potential respectively.

In conclusion, it is hoped that the addition of a vectorial method for the formation of Pi-terms to those proposed by the authors will add further clarity and physical understanding to dimensional analysis, and consequently to the determination of functional equations in the diversified fields of science.

REFERENCES

1. Birkhoff, G., Hydrodynamics, A Study in Logic, Fact, And Similitude, Princeton University Press, 1950.

2. Sarpkaya, T., "Vektörlerle Boyutsal Analiz", Yapi Teknik Mühendislik Dergisi, pp. 1-5, Sayi 4, Haziran 1954, (in Turkish).

M 2

q^n,

e
clari
to the

k